(2)

MASSACHUSETTS INSTITUTE OF TECHNOLOGY VLSI PUBLICATIONS

VLSI Memo No. 89-576
October 1989

Mechanical Properties of Microelectronics Thin Films: Silicon Nitride (Si_3N_4)

Fariborz Maseeh, Miles Arnone, and Stephen D. Senturia

Abstract

Mechanical design of microfabricated devices requires knowledge of mechanical material properties. Thin film material properties are sensitively process dependent, and should therefore be organized accordingly. A relational database of material properties is under development as part of a general micro-electro-mechanical ~~CAD~~ environment. A computerized literature search through the published values for Silicon Nitride (Si_3N_4) properties under various processing conditions resulted in the following document.

Microsystems Technology Laboratories
Massachusetts Institute of Technology
Cambridge Massachusetts 02139
Room 39-321
Telephone (617) 253-0292

Acknowledgements

This research was supported in part by the Defense Advanced Research Project Agency under contract number MDA-972-88-K-0008.

Author Information

Maseeh and Arnone: Department of Electrical Engineering & Computer Science, Room 39-665, MIT, Cambridge, MA 02139. (617) 253-0725.

Senturia: Department of Electrical Engineering & Computer Science, Room 39-665, MIT, Cambridge, MA 02139. (617) 253-6869.

DISCLAIMER NOTICE

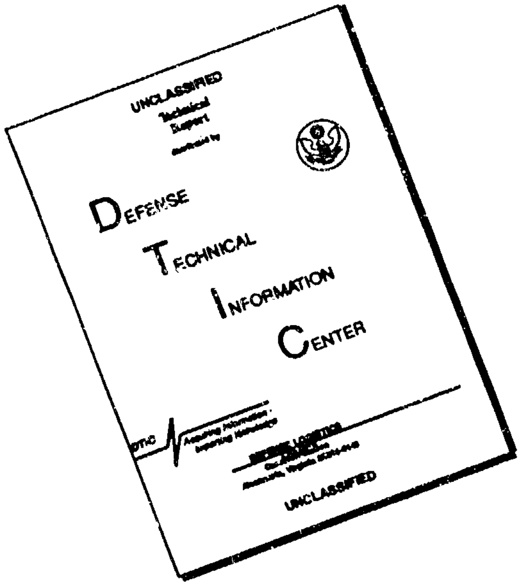

THIS DOCUMENT IS BEST QUALITY AVAILABLE. THE COPY FURNISHED TO DTIC CONTAINED A SIGNIFICANT NUMBER OF PAGES WHICH DO NOT REPRODUCE LEGIBLY.

PROPERTIES OF MICROELECTRONIC SILICON NITRIDE (Si_3N_4)

FARIBORZ MASEEH, MILES ARNONE, STEPHEN D. SENTURIA

MICROSYSTEMS TECHNOLOGY LABORATORIES
MASSACHUSETTS INSTITUTE OF TECHNOLOGY
DEPARTMENT OF ELECTRICAL ENGINEERING & COMPUTER SCIENCE
CAMBRIDGE, MA, USA

OCTOBER 1989

Sponsored by
Defense Advanced Research Projects Agency
DARPA/ISTO
"Computer-Aided Fabrication of Integrated Circuits"
ARPA Order No. 6510, PCN 8E20
Program Code No. BK0011
Issued by DARPA/CMO under Contract No.
MDA-972-88-k-0008.

Introduction

There is a growing need for the ability to perform mechanical analysis of microelectronic devices, both in assuring structural reliability against failure of thin film layers, and in evaluating the effects of various external loads including temperature and humidity effects. In addition, with the development of increasingly sophisticated micromechanical devices, including microsensors, pumps, valves, and micromotors, and with the increasing performance demands being placed on these devices, notably in the precision and accuracy of microsensors, there is a critical need for computer-aided-design (CAD) tools which will permit rational design of these devices. The present program is directed towards creation of a suitable CAD environment for micromechanical analysis of microfabricated deformable structures utilized for measuring the mechanical properties of thin films, and static analysis of which can be utilized for reliability investigations.

There are two fundamental problems that confront the designer [*,**]: (1) the need to construct a three- dimensional solid model from a description of the mask set and process sequence to be used in fabrication of a micromechanical device; and (2) the need to be able to predict the mechanical properties of each of the constituent materials in a device, including possible process dependences of these properties. With such a 3-D model in hand, with appropriate properties for each material, prediction of mechanical behavior could be done with existing finite-element modeling (FEM) programs. However, at the present time, there is no CAD system, either mechanical or microelectronic, which successfully addresses these problems in a coherent way. Koppelman [***] has developed a program called OYSTER which permits construction of a 3-D polyhedral-based solid model from a mask set and primitive process description, but as yet, there is no provision for linking to FEM tools or to standardly used layout and process modeling tools, and no database for prediction of mechanical properties from the process sequence.

An architecture for a micro-electro-mechanical CAD system in which these two critical problem areas can be the focus of simultaneous and parallel development work is presented in Fig. 1. The basic idea is to provide three different levels of user interaction: (1) at the conventional microelectronic level, with access to mask layout and process specification; (2) at the mechanical CAD level, for direct construction of 3-D solid models which can then be analyzed with FEM; and (3) at the mechanical-property database level, for entry of mechanical property data as it is acquired and documented. There are then two specific development tasks: (1) development of a 3-D solid modeling tool, which we call the "structure simulator", and which takes mask layout data and a realistic process description and builds a 3-D solid model in a format compatible with the mechanical CAD system (an extension of what OYSTER now does); and (2) the development of a mechanical property database using iterative measurements on deformable micromechanical structures (such as diaphragms, beams, and resonant structures) together with careful FEM studies of the dependence of their behavior on mechanical properties.

We have implemented this architecture in a Sun 4 host, drawing on existing codes wherever possible. The primary interface for mechanical modeling is through PATRAN, a mechanical CAD package which provides for manual construction of 3-D solid models, graphical display, and interfacing with FEM packages (we are using ABAQUS). The 3-D solid model resides in the PATRAN Neutral File, and we have elected to use the material-property format of the Neutral File as a first version of the Mechanical Property Database. Layout is provided through KIC, and process description through the process-flow representation (PFR) is created with a standard text editor. SUPREM III and SAMPLE are installed to provide depth and cross-sectional modeling capabilities. The structure simulator (under development) will accept KIC and PFR files as input, draw on SUPREM

III and SAMPLE as needed, and will output a 3-D solid model in the format of the PATRAN Neutral File. PATRAN will then be able to pick up the model, provide for FEM analysis and graphical display of behavior. The present status is that all of the commercially available codes (solid boxes in Fig. 1) are installed and operating. The first entries into the Mechanical Property Database have been made for silicon dioxide and silicon nitride as a result of the literature review enclosed.

This document is the result of a computerized literature search (done at MIT CLSS) to locate published mechanical property data for silicon nitride, Si_3N_4. Investigating some 100+ references, a group of 36 was selected and the mechanical properties of Si_3N_4 were extracted under different chemical vapor depositions (CVD) and sputter depositions. The cited values are arranged by different mecnanical property headings, and then by the deposition method as subheadings. The boldface values indicate results of experimental measurements (from references), and the italic values correspond to when a reference cites results from other references without measurements, or when no reference experiment was indicated to support the cited values. Most values were traced to their original measurement (experiment) when possible. Averages of the cited properties have been implemented in our mechanical properties database.

References

*. S. D. Senturia, "Microfabricated structures for the measurement of mechanical properties and adhesion of thin films", Transducers '87, Tokyo, 1987, pp. 11-16.

**. S. D. Senturia, "Can we design microrobotic devices without knowing the mechanical properties of materials?", IEEE MicroRobots and Teleoperators Workshop, Hyannis, 1987.

***. G. Koppelman, "OYSTER: a 3D structural simulator for microelectromechanical design," MEMS '89, Salt Lake City, 1989, pp. 88-93.

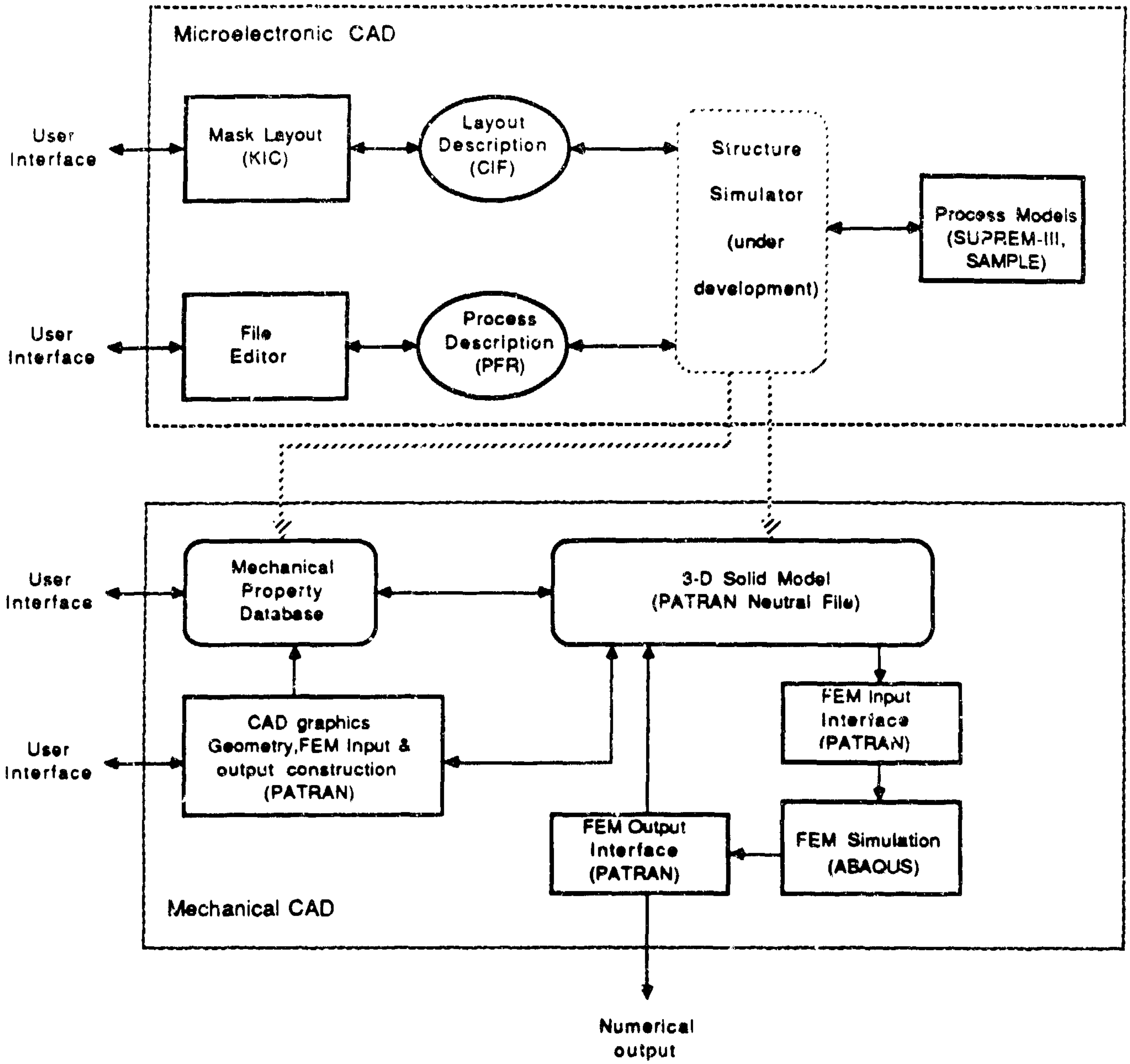

Fig. 1

CAD architecture for micro-electro-mechanical design

Table of Contents

Density

P.E.C.V.D.

Gas Flow - Density Relationships

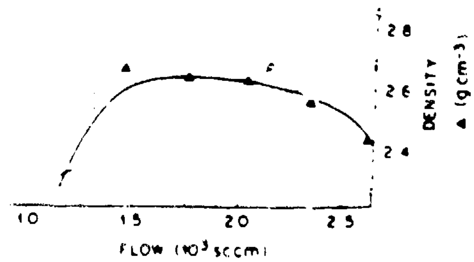

Fig. 1: Gas flow vs. film density.

Conditions: Gases: Ar, NH_3 and SiH_4;
SiH_4 concentration = 1.7 %; SiH_4/NH_3 = 0.71;
T = 275 C; P = 127 Pa; R.F. Power = 250 W
Taken from Sinha [31]

Density

P.E.C.V.D.

Gas Ratios and Composition - Density Relationships

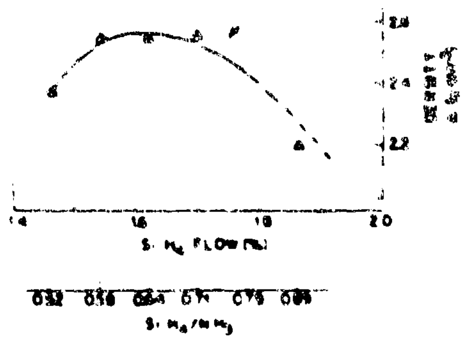

Fig. 2: Density vs. SiH_4/NH_3 and SiH_4 concentration.

Conditions: Gases: Ar, NH_3 and SiH_4;
SiH_4 concentration = 1.7 %; SiH_4/NH_3 = 0.71;
T = 275 C; P = 127 Pa; R.F. Power = 250 W
Taken from Sinha [31]

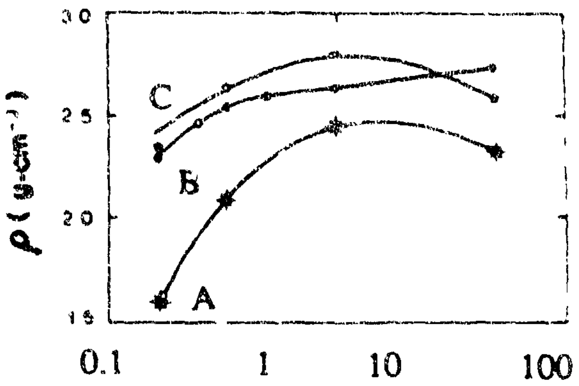

Fig. 3: Effect of NH_3/SiH_4 upon density.

Conditions:
A: ϕ_{N2} = 90 sccm; ϕ_{NH3} = 50 sccm;
R.F. power = 1 kW; P = 33 Pa; T = 200 C

B: ϕ_{NH3} = 50 sccm; R.F. power = 1 kW;
P = 33 Pa; T = 200 C

C: ϕ_{Ar} = 90 sccm; ϕ_{NH3} = 50 sccm;
R.F. power = 1 kW; P = 33 Pa; T = 200 C

Taken from Tessier [33]

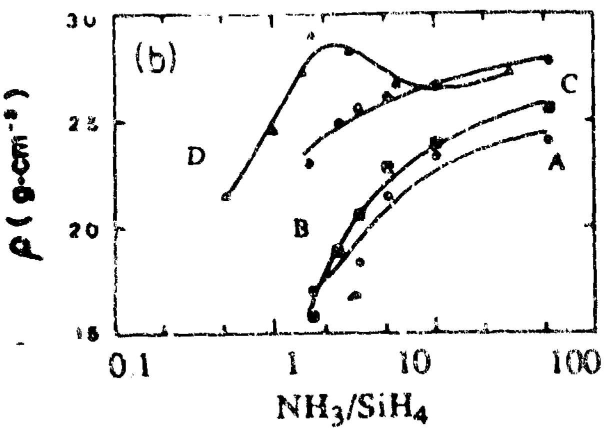

Fig. 4: Effect of NH_3/SiH_4 upon density.

Conditions: Gases: N_2, NH_3 and SiH_4;
ϕ_{NH3} = 50 sccm, R.F. power = 1 kW; P = 33 Pa
A: T = 25 C
B: T = 100 C
C: T = 200 C
D: T = 250 C
Taken from Tessier [33]

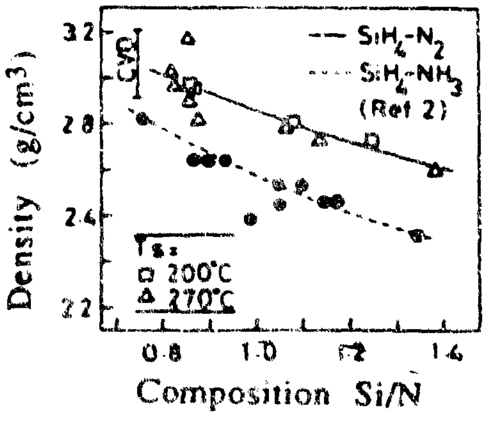

Fig. 5: Effect of Si/N composition upon density.

Conditions: Gases: N_2 and SiH_4
R.F. power = 0.64W/cm^2; P = 267 Pa,
T = 270 C
Taken from Zhou [36]

Density

P.E.C.V.D.

R.F. Frequency - Density Relationships

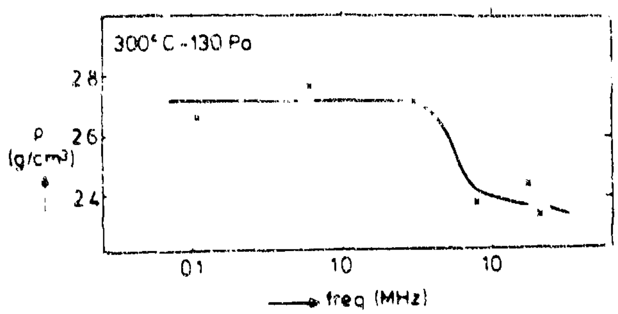

Fig. 6: Relationship between R.F. frequency and density.
P = 130 Pa; T = 300 C; R.F. power = 50 W;
ϕ_{SiH4}=100 sccm; ϕ_{N2}=700 sccm; ϕ_{NH3}=700 sccm.
Taken from Claassen [5].

Density

P.E.C.V.D.

R.F. Power - Density Relationships

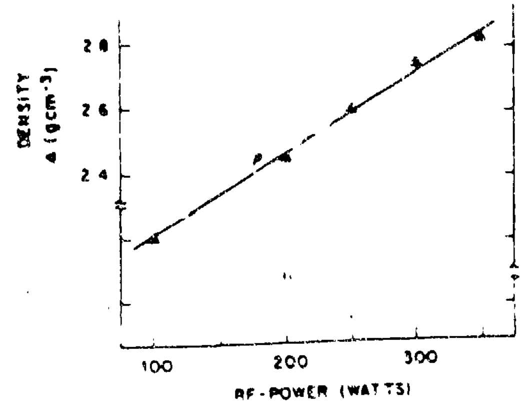

Fig. 7: Effect of R.F. power upon density.
Reacting gases SiH_4, NH_3 and Ar; T = 275 C;
SiH_4 conc. = 1.78 %; SiH_4/NH_3 = 0.79
Gas flow = 2320 sccm; R.F. Power = 300 W;
P = 127 Pa
Taken from Sinha [31].

Density

P.E.C.V.D.

Pressure - Density Relationships

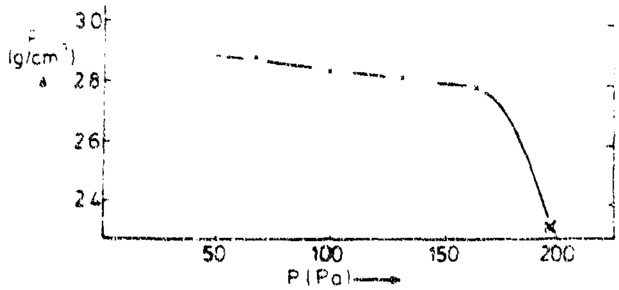

Fig. 8: Efect of increased pressure upon density.

Conditions: Gases: N_2, NH_3 and SiH_4; ϕ_{N2} = 300 sccm; ϕ_{NH3} = 1100 sccm; ϕ_{SiH4} = 100 sccm; R.F. frequency = 310 kHz; R.F. power = 50 W; T = 300 C
Taken from Claassen [5]

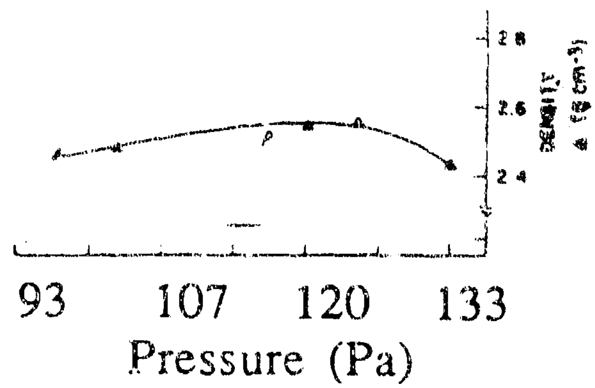

Fig 9: Relation between gas pressures and density.

Conditions: Gases: Ar, NH_3 and SiH_4;

SiH_4 concentration = 1.78 %; SiH_4/NH_3 = 0.71; ϕ =2320 sccm; T = 275 C; R.F. Power = 250 W
Taken from Sinha [31]

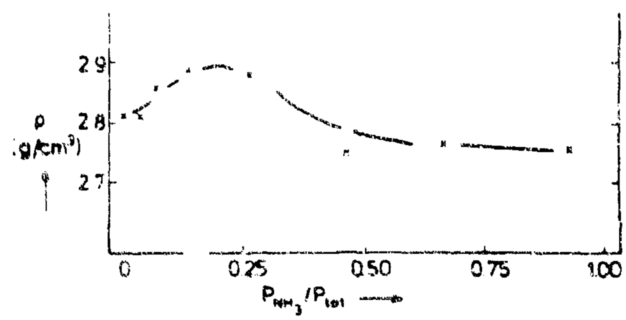

Fig. 10: Relation between pressure and density.

Conditions: Gases: N_2, NH_3 and SiH_4.

ϕ_{NH3+N2} = 1400 sccm; ϕ_{SiH4} = 100 sccm;
R.F. frequency = 310 kHz; R.F. power = 50 W;
P = 65 Pa; T = 300 C
Taken from Claassen [5]

Density

P.E.C.V.D.

Temperature - Density Relationships

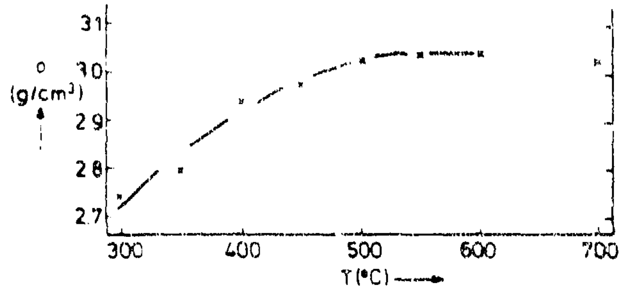

Fig. 11: Density as a function of temperature.

Conditions: Gases: N_2, NH_3 and SiH_4; ϕ_{N2} = 200 sccm;
ϕ_{NH3} = 1200 sccm; ϕ_{SiH4} = 100 sccm;
R.F. frequency = 310 kHz; R.F. power = 50 W;
P = 130 Pa
Taken from Claassen [5]

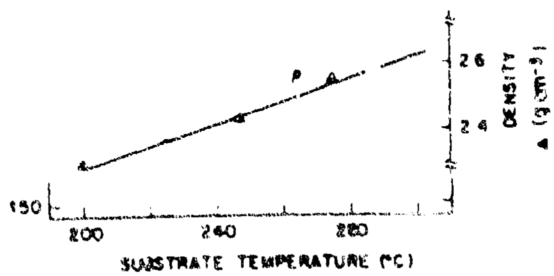

Fig. 12: Effect of substrate temperature upon density.

Conditions: Gases: Ar, NH_3 and SiH_4;
SiH_4 concentration = 1.7 %; SiH_4/NH_3 = 0.71;
P = 127 Pa; R.F. Power = 250 W
Taken from Sinha [31]

Density

P.E.C.V.D.

Density Values

2.55 (g/cm^3) [19]

Conditions: Plasma Technology Model 80 Reactor.
Taken from Kember [19]

3.02 - 3.21 (g/cm^3) [8]

Conditions: Gases: H_2, NH_3 and SiH_4; ϕ_{H2} = 4 liters/min.;
SiH_4/NH_3 = 1 to 20 - 40; T = 750 - 1100 C
Taken from Doo [8]

2.7 +/- 0.10 (g/cm^3) [7]

Conditions: Gases: N_2, NH_3 and SiH_4 (2%); ϕ_{N2} = 1375 cm^3/min;
ϕ_{NH3} = 6 cm^3/min; ϕ_{SiH4} = 35 cm^3/min; R.F. Power = 400 W;
R.F. Frequency = 50 kHz; P = 33.3 Pa; T = 325 C
Taken from Dharmadhikari [7]

2.5 +/- 0.10 (g/cm^3) [7]

Conditions: Gases: N_2, NH_3 and SiH_4 (100%); ϕ_{N2} = 1000 cm^3/min;
ϕ_{NH3} = 400 cm^3/min; ϕ_{SiH4} = 150 cm^3/min; R.F. Power = 400 W;
R.F. Frequency = 50 kHz; P = 26.7 Pa; T = 325 C
Taken from Dharmadhikari [7]

Density

Various Depositions

Density Values

Table 1: Typical density values for various depositions as reported by Morosanu in his review of the literature. [26]

Preparation method	*Density* ($g\ cm^{-3}$)
CVD. $SiH_4 + NH_3$	2.75-3.11
CVD. $SiCl_4 + NH_3$	3.1
CVD. $SiH_4 + N_2H_4$	3-3.1
CVD. $SiH_2Cl_2 + NH_3$	3.1
RFGD. $SiH_4 + NH_3$	
RFGD. $SiH_4 + N_2$	
LPCVD. $SiH_4 + NH_3$	
LPCVD. $SiH_2Cl_2 + NH_3$	
Direct r.f. sputtering	3
Reactive r.f. sputtering	2.8-3
CVD. $Si_xO_yN_z$	2.1-3.1

Density

Sputtering

2.8 - 3.0 (g/cm^3) [26].

Conditions: The deposition conditions are not elaborated upon. Taken from Morosanu [26]

Bulk Material

3.2 (g/cm^3) [23].

Elastic Stiffness

C.V.D.

Thermal Expansion Coefficient - Elastic Modulus Relationships

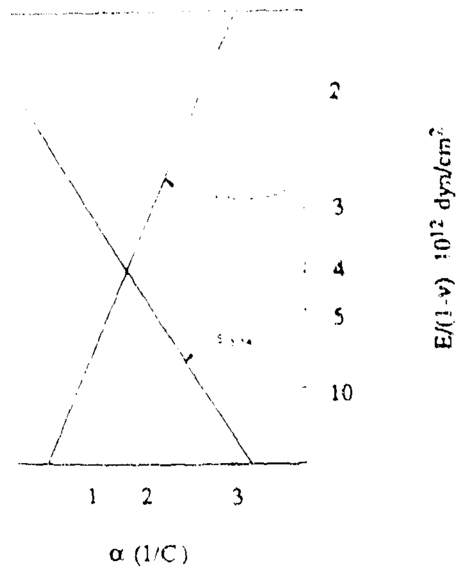

Fig. 1: Elastic stiffness as a function of thermal expansion coefficient for quartz and silicon substrates.

Conditions: Nitrox Reactor at 800 C.
Taken from Retaajczyk [29]

Elastic Stiffness (Biaxial Modulus)

C.V.D.

Elastic Stiffness Values

3.7×10^{12} (dyn/cm^2) [29].

Conditions: Nitrox Reactor; T = 800 C, thickness = 2000 angstroms [29]

A.P.C.V.D.

Elastic Stiffness Values

1.5×10^{12} (dyn/cm^2) [27].

Conditions: Gases: SiH_4, NH_3 and Ar; SiH_4/NH_3 = 0.2;
Net gas flow is constant; P = 133 Pa;
T = 700 - 800 C [27]

P.E.C.V.D.

Elastic Stiffness Values

3×10^{12} (dyn/cm^2) [14].

Conditions: Gases: SiH_4, NH_3 and N_2; 1% SiH_4 in N_2;
NH_3/SiH_4 > 10; T = 700 -1000 C [14]

Fracture

P.E.C.V.D.

Annealing - Fracture Relationships

Doo [8] found that cracks occur in films thicker than one micron that have been annealed.

Conditions: Gases: H_2, NH_3 and SiH_4; ϕ_{H2} = 4 liters/min;
SiH_4/NH_3 = 1 to 20 - 40; T = 750 - 1100;
Annealed for 15 minutes at 1200 C
Taken from Doo [8]

Isomae [16] found the following relationship for the force required to initiate fracture in annealed films:

$$F_f = 10.5 \exp(Q/kT)$$

T = annealing temperature; $600 < T < 1200$ C
Q = 0.25 eV

Conditions: Gases: N_2, NH_3 and SiH_4;
SiH_4/NH_3 = 0.007; T = 950;
Taken from Isomae [16]

Fracture

P.E.C.V.D.

Crack Resistance

Kember [19] observed a crack resistance of less than 500 C in nitride thin films.

Conditions: Plasma Technology Model PD80 Reactor
Taken from Kember [19]

Fracture

P.E.C.V.D.

Density - Fracture Relationships

Sinha [31] observed brittle behavior in films with low densities.

Conditions: Gases: Ar, NH_3 and SiH_4;SiH_4 conc. = 1.7%;
SiH_4/NH_3 = 0.71; ϕ = 2320 sccm; P = 127 Pa; T = 275 C
Taken from Sinha [31]

Fracture

P.E.C.V.D.

Thickness - Fracture Relationships

Tamura [32] observed cracking in films with thicknesses over one half micron.

Conditions: Gases: N_2, NH_3 and SiH_4; ϕ_{NH3} = 1000 cc/min;
T = 940 C;
Taken from Tamura [32]

Poisson's Ratio

Sputtering

Poisson's Ratio Values

0.25 [25].

Conditions: Gases: H_2, N_2 and Ar; Si/N = 0.75 - 7;
Power density = 3.20 W/cm^2 [25]

Bulk Material

Poisson's Ratio Values

0.27 - 0.28 [23].

Refractive Index

L.P.C.V.D.

Gas Flow - Refractive Index Relationships

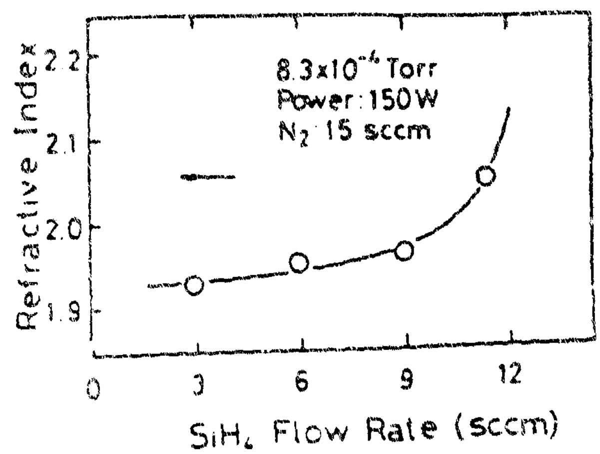

Fig. 1: The effect of increased SiH_4 flow rate upon refractive index. (L.P.C.V.D.)

Conditions: Gases: SiH_4 and N_2; ϕ_{N2} = 15 sccm;
R.F. power = 150 W; P = 0.12 Pa
Taken from Hirao [13]

Refractive Index

L.P.C.V.D.

Residual Stress - Refractive Index Relationships

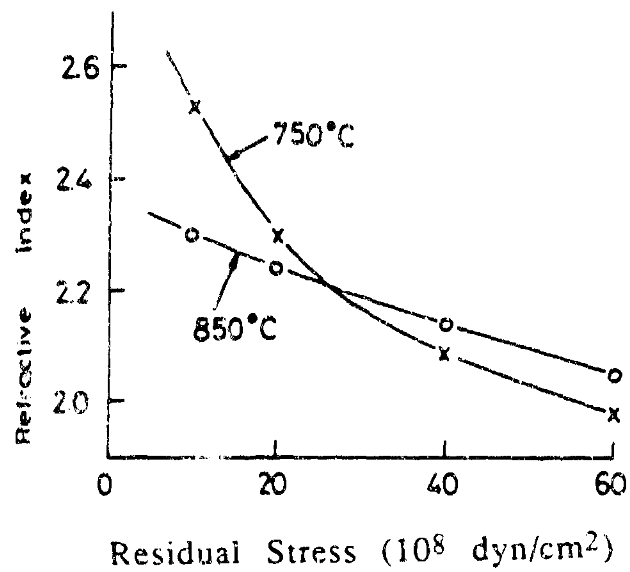

Fig. 2: Relation between residual stress(tensile) and Refractive Index.

Conditions: Gases: NH_3 and SiH_2Cl_2; P = 66.75 Pa;
T = 750, and 850 C
Taken from Sekimoto [30]

Refractive Index

L.P.C.V.D.

R.F. Power - Refractive Index Relationships

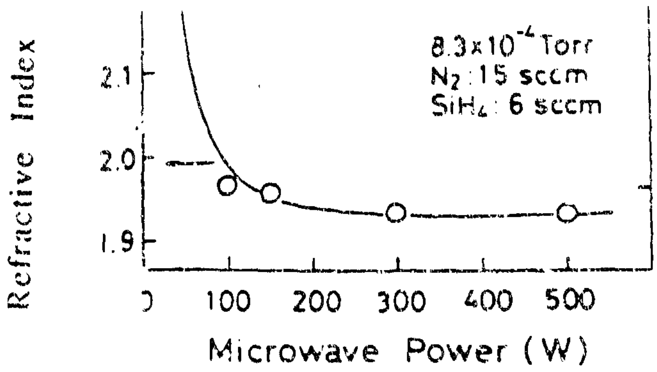

Fig. 3: Effect of R.F. power on Refractive index.

Conditions: Gases: SiH_4 and N_2; Φ_{N2} = 15 sccm; Φ_{SiH4} = 6 sccm; P = 0.12 Pa
Taken from Hirao [13]

Refractive Index

L.P.C.V.D.

Pressure - Refractive Index Relationships

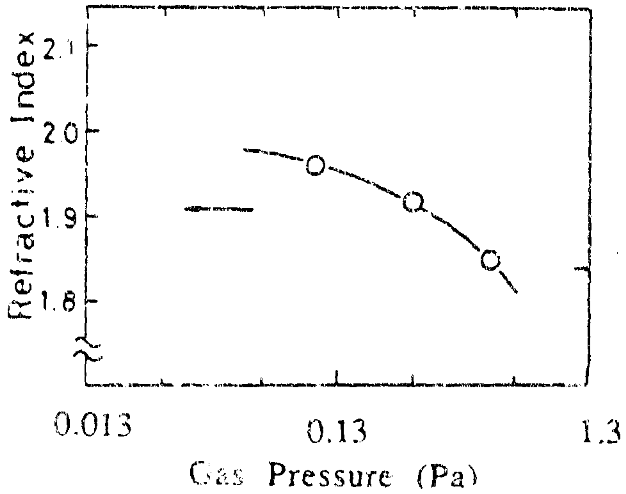

Fig 4: Effect of gas pressure upon Refractive index.

Conditions: Gases: SiH_4 and N_2; ϕ_{N2} = 15 sccm;
ϕ_{SiH4} = 6 sccm; R.F. power = 150 W
Taken from Hirao [13]

L.P.C.V.D.

Refractive Index

Refractive Index Values

1.99 +/- 0.02 [28].

<u>Conditions</u>: Gases: NH_3 and SiH_2Cl_2; $\phi_{SiH2Cl2}$ = 15 sccm; T = 770 C [28]

Refractive Index

A.P.C.V.D.

Refractive Index Values

1.95 - 1.96 [27].

Conditions: Gases: Ar, NH_3 and SiH_4; $SiH_4/NH_3 = 0.2$;
Net gas flow is constant; P = 133 Pa; T = 650 - 850 C [28]

1.98 - 1.99 [27].

Conditions: Gases: Ar, NH_3 and SiH_4; $SiH_4/NH_3 = 0.2$;
Net gas flow is constant; P = 133 Pa; T = 650 - 850 C;
Annealed at 1000 C [28]

Refractive Index

P.E.C.V.D.

Annealing - Refractive Index Relationships

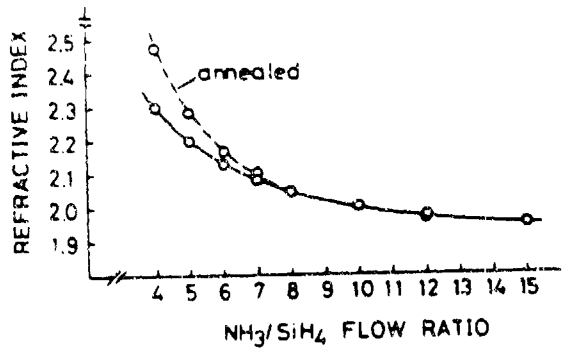

Fig. 5: The effect of annealing upon refractive index.

Conditions: Gases: NH_3 and SiH_4; R.F. frequency = 400 kHz;
R.F. power = 26 - 100 W; P = 267 Pa; T = 200, 380 C
Taken from Ishii [15]

Refractive Index

P.E.C.V.D.

Gas Flow - Refractive Index Relationships

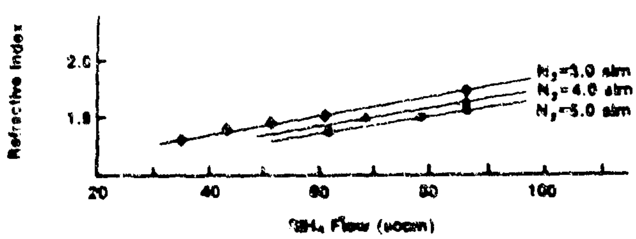

Fig. 6: The effect of SiH_4 flow on refractive index.

Conditions: Gases: N_2, NH_3 and SiH_4; R.F. frequency = 13.56 MHz; R.F. power = 300 - 500 W; P = 267 - 668 Pa; T = 260 - 400 C
Taken from Chang [3].

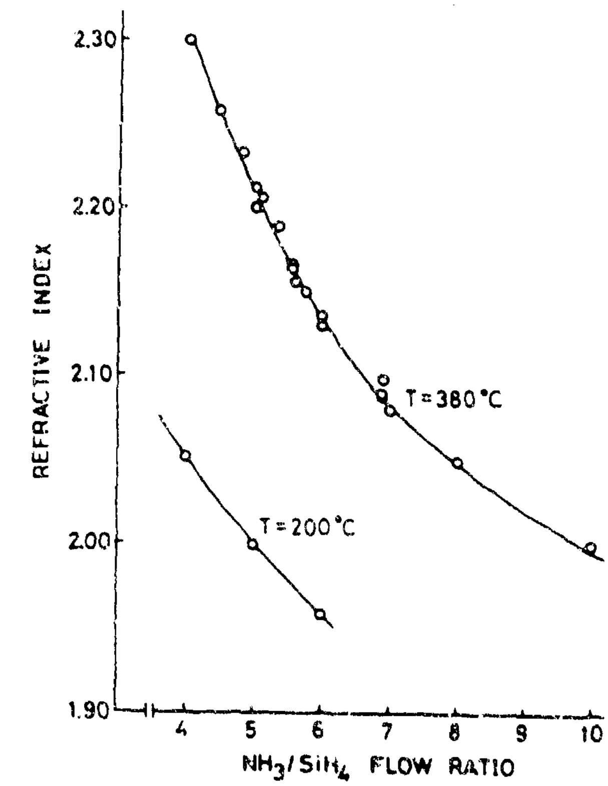

Fig. 7: Dependance of refractive index upon NH_3/SiH_4 flow ratio

Conditions: Gases: NH_3 and SiH_4; R.F. frequency = 400 kHz; R.F. power = 26 - 100 W; P = 267 Pa; T = 200, 380 C
Taken from Ishii [15]

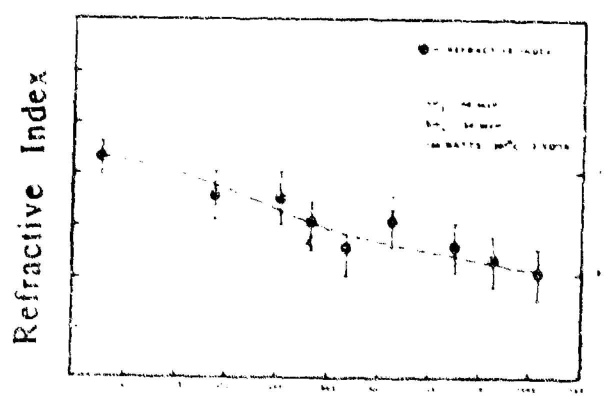

Fig. 8: Refractive index as a function of nitrogen flow.

Conditions: Gases: N_2, NH_3 and SiH_4; Φ_{NH3} = 40 sccm; Φ_{SiH4} = 30 sccm; R.F. power = 100 W; P = 267 Pa; T = 300 C
Taken from Khanq [20]

Refractive Index

P.E.C.V.D.

Gas Flow - Refractive Index Relationships

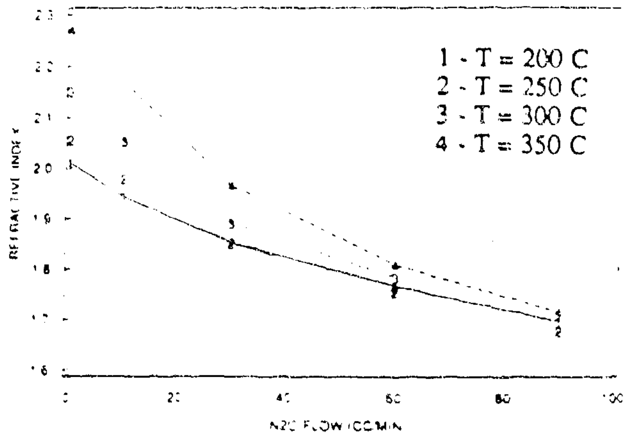

Fig. 9: Refractive Index vs. N_2O flow.

Conditions: N_2, N_2O and NH_3; ϕ_{SiH4} (in N2) = 2950 cm^3/min;
R.F. frequency = 380 kHz; R.F. power = 700 W; P = 48 Pa
Taken from Knolle [21]

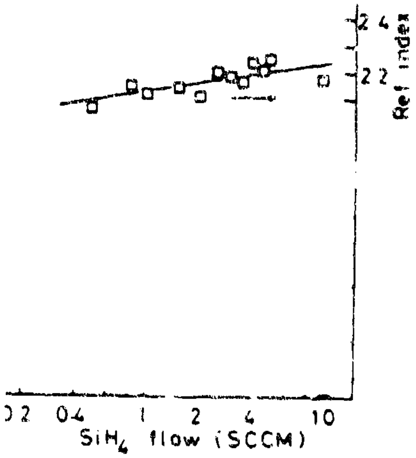

Fig. 10: Refractive index as a function of SiH4 flow rate.

Conditions: Gases: N_2 and SiH_4; ϕ_{N2} = 30 sccm;
R.F. frequency = 13.56 MHz; R.F. power = 0.64 W/cm^2;
P = 53.3 Pa; T = 270 C
Taken from Zhou [36]

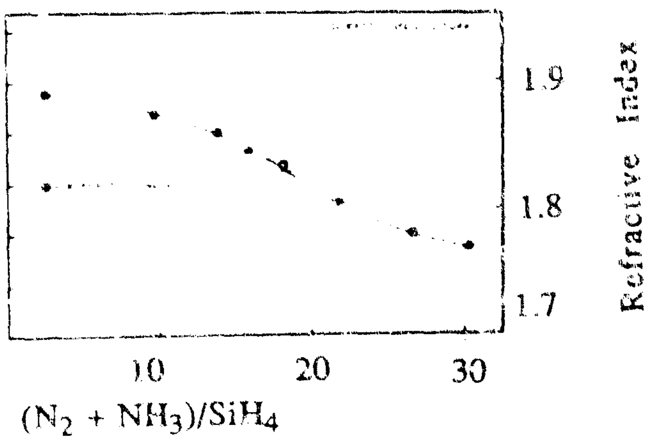

Figure 11: Refractive index as a function of gas ratio.

Conditions: Gases: N_2, NH_3, and SiH_4, R.F. Frequency = 13.56 MHz,
R.F. power = 100 W, P = 267 Pa; T = 300 C
Taken from Khaliq [20]

Refractive Index

P.E.C.V.D.

Gas Flow - Refractive Index Relationships

Table 1: Refractive index as a function of N_2O flow and Temperature

N_2O flow (cm^3/min)	Temp. (C)	Refractive index
0	200	2.01
10	200	1.94
30	200	1.85
60	200	1.77
90	200	1.70
0	250	2.06
10	250	1.98
30	250	1.85
60	250	1.75
90	250	1.68
0	300	2.15
10	300	2.05
30	300	1.89
60	300	1.78
0	350	2.27
10	350	1.97
20	350	1.81

<u>Conditions</u>: N_2, N_2O and NH_3; ϕ_{SiH4} (in N2) = 2950 cm^3/min;
R.F. frequency = 380 kHz; R.F. power = 700 W; P = 48 Pa
Taken from Knolle [21]

Refractive Index

P.E.C.V.D.

Gas Ratio - Refractive Index Relationships

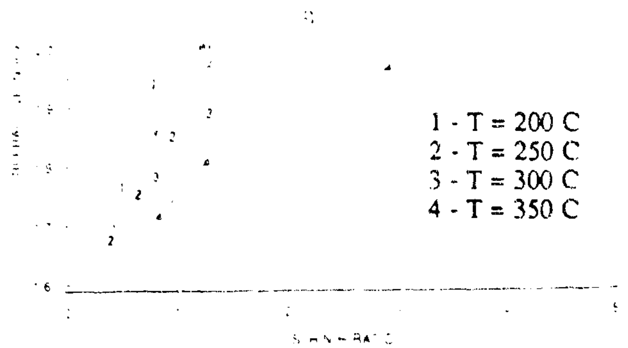

Figure 12: Refractive index as a function of Si-N/N-H ratio.

Conditions: N_2, N_2O and NH_3; ϕ_{SiH4} (in N2) = 2950 cm^3/min; R.F. frequency = 380 kHz; R.F. power = 700 W; P = 48 Pa
Taken from Knolle [21]

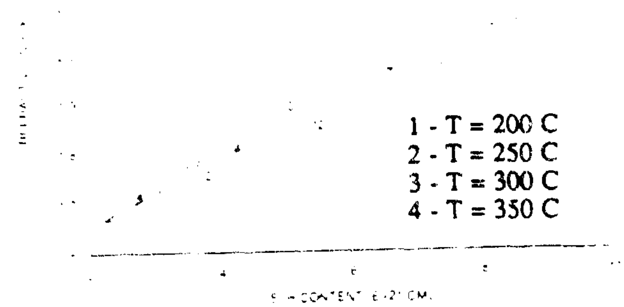

Fig. 13: Refractive index vs. Si-H content.

Conditions: N_2, N_2O and NH_3; ϕ_{SiH4} (in N2) = 2950 cm^3/min; R.F. frequency = 380 kHz; R.F. power = 700 W; P = 48 Pa
Taken from Knolle [21]

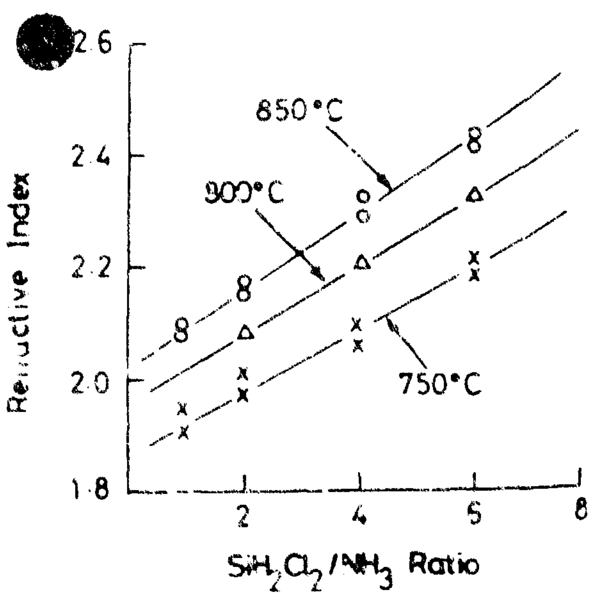

Fig. 14: Refractive index vs. SiH_2Cl_2/NH_3 ratio.

Conditions. Gases: NH_3 and SiH_2Cl_2; P = 66.75 Pa
T = 750, 800 and 850 C
Taken from Sekimoto [30]

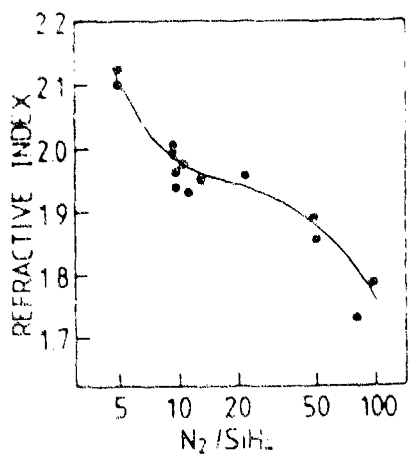

Fig. 15: Effect of gas composition on Refractive index.

Conditions: H_2, N_2 and SiH_4; ϕ_{SiH4} (in N2) = 2950 cm^3/min; R.F. frequency = 13.56 MHz; R.F. power density = 0.8 W/cm^2; P = 400 - 933 Pa; T = 300 C
Taken from Watanabe [35]

Refractive Index

P.E.C.V.D.

Gas Ratio - Refractive Index Relationships

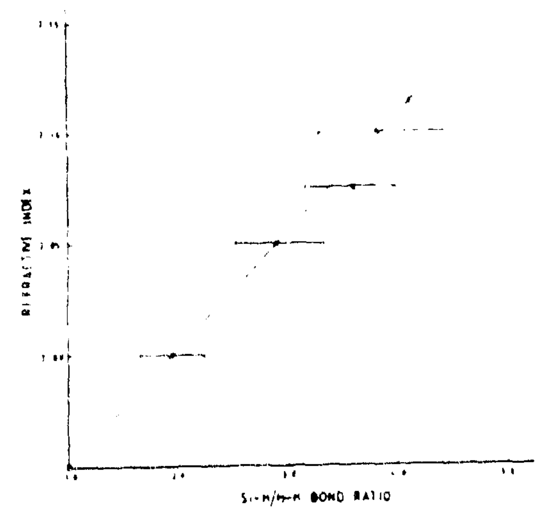

Fig. 16: Refractive index as a function of Si-N/N-H bond ratio

Conditions: Plasma Technology Model PD80 Reactor
Taken from Kember [19]

Refractive Index

P.E.C.V.D.

R.F. Power - Refractive Index Relationships

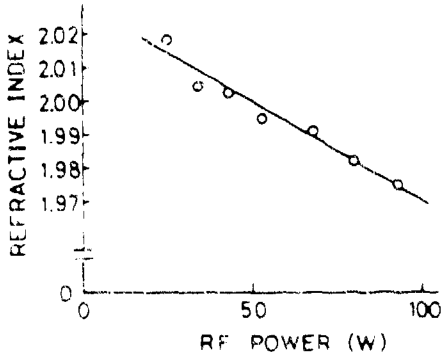

Fig. 17: Effect of R.F. power on Refractive index.

Conditions: Gases: NH_3 and SiH_4; R.F. frequency = 400 kHz;
R.F. power = 26 - 100 W; P = 267 Pa; T = 200, 380 C
Taken from Ishii [15]

Refractive Index

P.E.C.V.D.

Position - Refractive Index Relationships

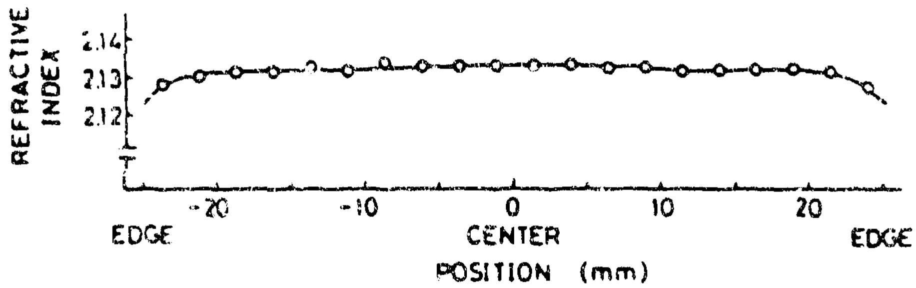

Fig. 18: Refractive index as a function of position
across a 5 cm wafer.

Conditions. Gases: NH_3 and SiH_4; R.F. frequency = 400 kHz;
R.F. power = 26 - 100 W; P = 267 Pa; T = 200, 380 C
Taken from Ishii [15]

Refractive Index

P.E.C.V.D.

Pressure - Refractive Index Relationships

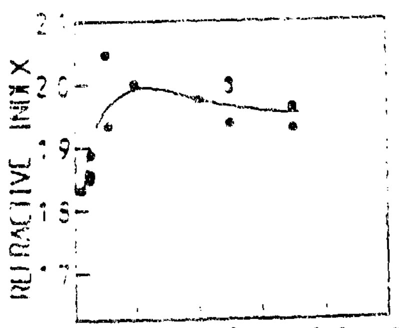

Fig. 19: Effect of gas pressure upon Refractive index.

Conditions: H_2, N_2 and SiH_4; ϕ_{SiH4} (in N2) = 2950 cm^3/min; R.F. frequency = 13.56 MHz; R.F. power density = 0.8 W/cm^2; T = 300 C
Taken from Watanabe [35]

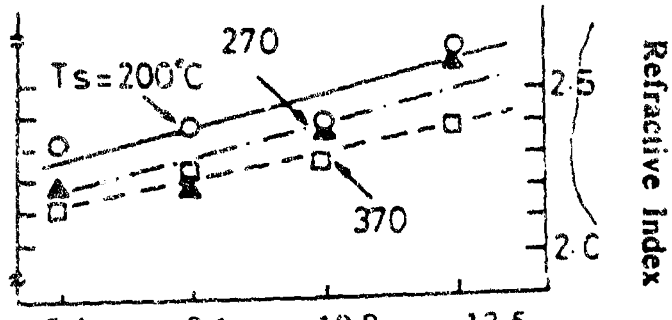

Fig. 20: Relationship between gas pressure and Refractive index.

Conditions: Gases: N_2 and SiH_4; ϕ_{N2} = 30 sccm; ϕ_{SiH4} = 30 sccm; R.F. frequency = 13.56 MHz; R.F. power = 0.64 W/cm^2; T = 270 C
Taken from Zhou [36]

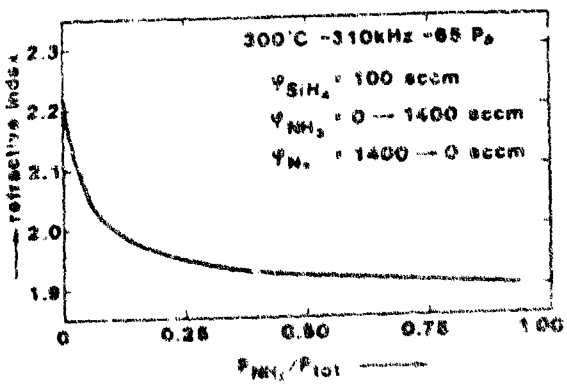

Fig. 21: Relationship between NH_3 gas pressure and Refractive index

Conditions: Gases: N_2, NH_3 and SiH_4; R.F. Frequency = 310 KHz; P = 65 Pa, T = 300 C
Taken from Claassen [5]

Refractive Index

P.E.C.V.D.

Temperature - Refractive Index Relationships

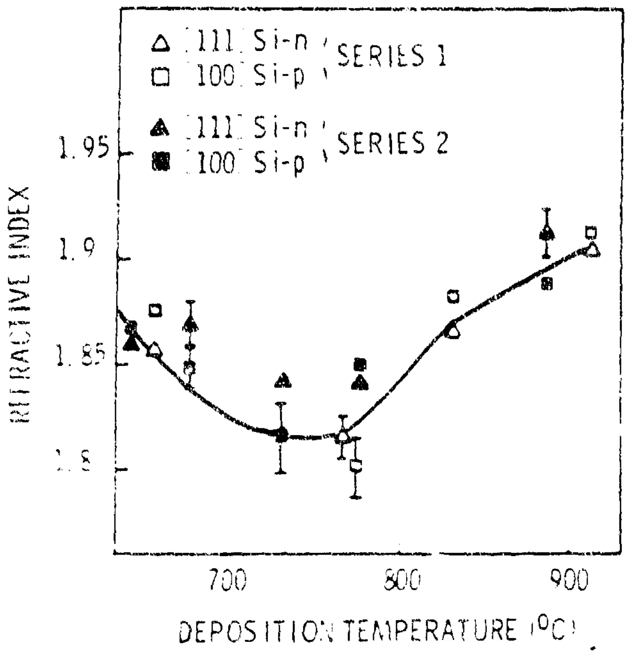

Fig. 22: Relationship between temperature and Refractive index.

Conditions: Gases: N_2, NH_3 and SiH_4; NH_3/SiH_4 = 1000
Taken from Hezel [12]

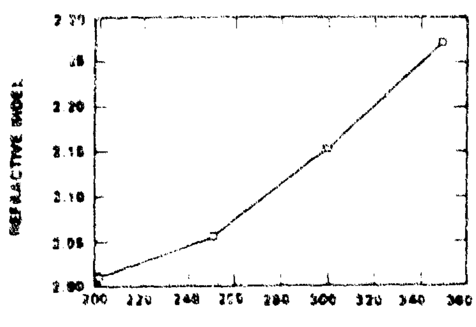

Fig. 23: Refractive index as a function of deposition temperature.

Conditions: N_2, N_2O and NH_3; ϕ_{SiH4} (in N2) = 2950 cm^3/min;
R.F. frequency = 380 kHz; R.F. power = 700 W; P = 48 Pa
Taken from Knolle [21]

Refractive Index

P.E.C.V.D.

Refractive Index Values

Table 2: Refractive index as a function of deposition characteristics. [18]

System	f(Hz)	P_d (W cm^{-2})	T_s(°C)	P(T)	Gas Flow (sccm) SiH_4	Gas Flow (sccm) NH_3	G_R(Å/min)	n
			120				170	1.98
A	13.56 M	0.04	260	0.3	?	?	175	2.02
			380				150	2.00
			100				290	1.83
B	13.56 M	0.38	250	0.5	22	80	310	--
			370				320	2.09
			100				159	1.78
C	13.56 M	0.02	275	0.32	17	120	90	1.94
			320				--	1.85
			400				81	2.02
			100				140	--
D	187.5 k	0.06	250	0.45	1400	--	112	--
			350				141	--
		150 W	100	0.6	380	1130	100	2.03
			250	0.73	380	1705	89	--
E1	50 k	235 W	380	1.49	365	2735	223	--
			500	2.0	255	2945	218	2.08
			100	0.6	380	1130	203	2.05
E2	450 k	150 W	380	1.49	365	2735	212	2.05
			500	2.0	245	2945	204	2.12
		300 W	100			700	254	2.15
		250 W	250			1525	239	--
F1	50 k	300 W	380	2.1	333	2000	311	--
		200 W	600			2400	398	--
		300 W	100			700	288	--
F2	450 k		380	2.1	333	2000	309	--
		200 W	600			2400	369	--

Refractive Index

Refractive Index

P.E.C.V.D.

Refractive Index Values

2.0 - 2.06 [8].

Conditions: Gases: H_2, NH_3 and SiH_4; ϕ_{H2} = 4 liters/min;
SiH_4/NH_3 = 1 to 20 - 40; T = 750 - 1100
Taken from Doo [8]

2.05 [19].

Conditions: Plasma Technologies Model PD80 Reactor
Taken from Kember [19]

1.95 +/- 0.028 [7].

Conditions: Gases: N_2, NH_3 and SiH_4 (2%); ϕ_{N2} = 1375 cm^3/min;
ϕ_{NH3} = 6 cm^3/min; ϕ_{SiH4} = 35 cm^3/min;R.F. power = 400 W;
R.F. frequency = 50 kHz; P = 26.7 Pa; T = 325 C
Taken from Dharmadhikari [7]

2.03 +/- 0.030 [7].

Conditions: Gases: N_2, NH_3 and SiH_4 (100%); ϕ_{N2} = 1000 cm^3/min;
ϕ_{NH3} = 400 cm^3/min; ϕ_{SiH4} = 150 cm^3/min;R.F. power = 400 W;
R.F. frequency = 50 kHz; P = 26.7 Pa; T = 325 C
Taken from Dharmadhikari [7]

Refractive Index

Various Depositions

Refractive Index Values

Table 3: Typical refractive index values as reported by Morosanu in a review of other literature. [26]

Preparation method	*Refractive index*
CVD. $SiH_4 + NH_3$	1.9-2.6
CVD. $SiCl_4 + NH_3$	2.0-2.8
CVD. $SiH_4 + N_2H_4$	2.0-2.1
CVD. $SiH_2Cl_2 + NH_3$	1.9-2.1
RFGD. $SiH_4 + NH_3$	1.9-2.8
RFGD. $SiH_4 + N_2$	2-2.5
LPCVD. $SiH_4 + NH_3$	1.98-2.08
LPCVD. $SiH_2Cl_2 + NH_3$	2.00
Direct r.f. sputtering	1.9-2.08
Reactive r.f. sputtering	2-2.1
CVD. $Si_xO_yN_z$	1.44-2.03

Residual Stress

L.P.C.V.D.

Gas Ratio - Residual Stress Relationships

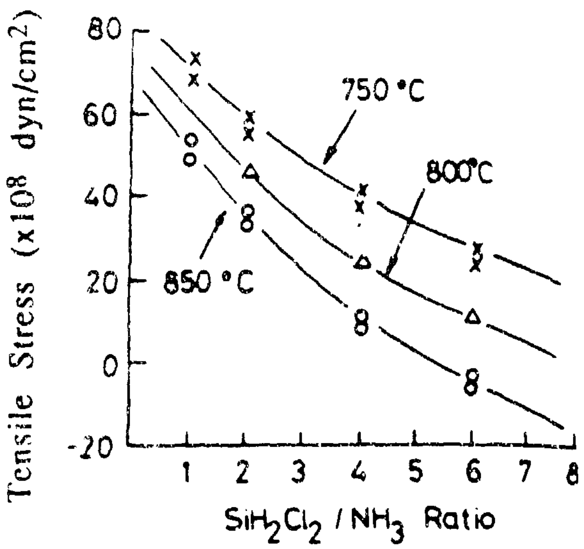

Fig. 1: Residual stress vs. SiH_2Cl_2/NH_3 ratio.

Conditions: Gases: NH_3 and SiH_2Cl_2; P = 66.75 Pa;
T = 750, 800 and 850 C
Taken from Sekimoto [30]

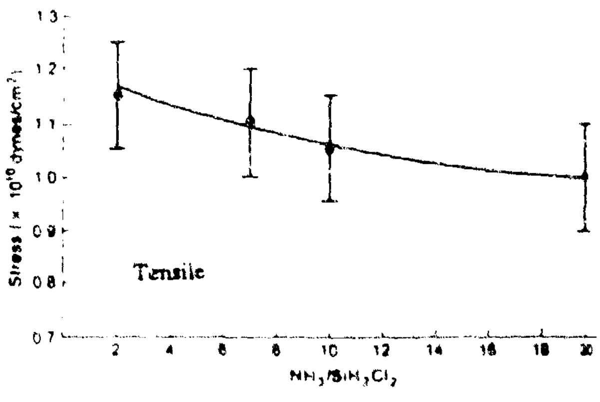

Fig. 2: Residual stress vs NH_3/SiH_2Cl_2 ratio.

Conditions: Gases: NH_3 and SiH_2Cl_2: $\Phi_{SiH2Cl2}$ = 15 sccm
Taken from Pan [28]

Residual Stress

L.P.C.V.D.

Residual Stress Values

Table 1: Residual stress and change in residual stress as a function of deposition conditions. [9]

NO/SiH_4	$n_N/(n_O+n_N)$	Atomic Fraction Si	T (cm × 10[illegible])	t (Å)	Days after prep.	Av R (m)	σ (dyn × 10^{-7}/cm²)	$\Delta\sigma \times 10^{-7}$ 60-day change
100	0	0.33	17.91	6750	4	31.5	−57.7	
					35	17.5	−104	
					63	14.3	−127	−69
30	0.067	0.34	6.27	5500	2	7.81	−35.1	
					4	6.36	−43.1	
					28	4.81	−57.0	
					46	4.21	−65.1	
					64	3.83	−71.6	−37
20	0.128	0.34_2	6.27	6000	0	20.9	10.9	
					1	23.6	9.7	
					3	49.8	4.6	
					8	46.2	4.9	
					17	66.9	3.4	
					30	70.3	3.2	
					48	174	1.3	
					66	174	1.3	−9.6
15	0.17	0.34	3.43	3750	4	2.40	50	
					11	3.65	33	
					35	5.10	24	
					62	8.46	14	−36
3	0.33	0.34_4	7.80	3400	4	5.34	128	
					35	5.86	117	
					63	5.18	132	4
1	0.42	0.38	7.80	2875	4	6.63	122	
					35	6.43	126	
					63	6.40	127	5
—*	1	0.43	8.38	2300	1	1.34	880	
					60	1.34	880	nil

* Pyrolytic Si_3N_4 from SiH_4+NH_3

__Conditions__: **Gases**: N_2, NH_3 and SiH_4; T = 850 C

Taken from Drum [9]

Residual Stress

C.V.D.

Annealing - Residual Stress Relationships

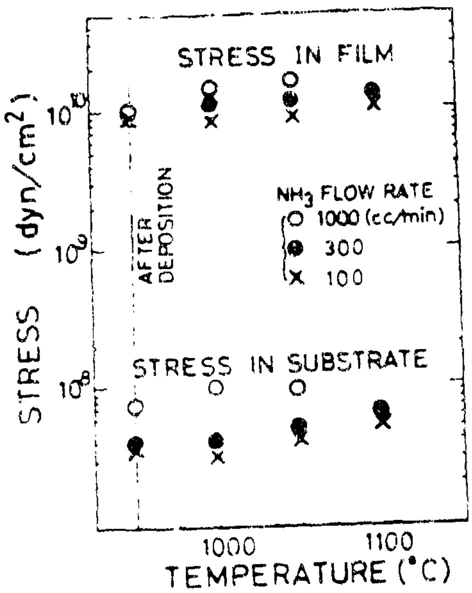

Fig. 3: Residual stress vs. annealing temperature.

Conditions: Gases: N_2, NH_3 and SiH_4;
T = 940 C
Taken from Tamura [32]

Residual Stress

C.V.D.

Gas Flow - Residual Stress Relationships

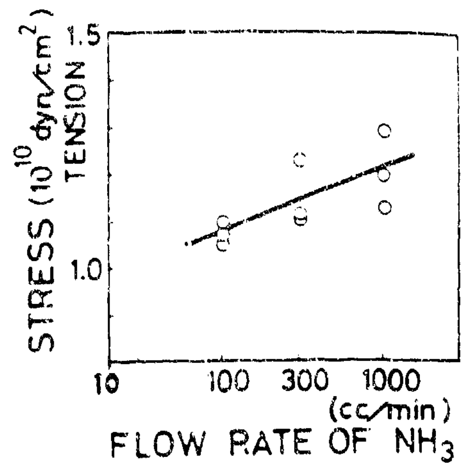

Fig. 4: Effect of NH_3 flow upon residual stress.

Conditions: Gases: N_2, NH_3 and SiH_4;
T = 940 C
Taken from Ta' ıura [32]

Residual Stress

C.V.D.

Temperature - Residual Stress Relationships

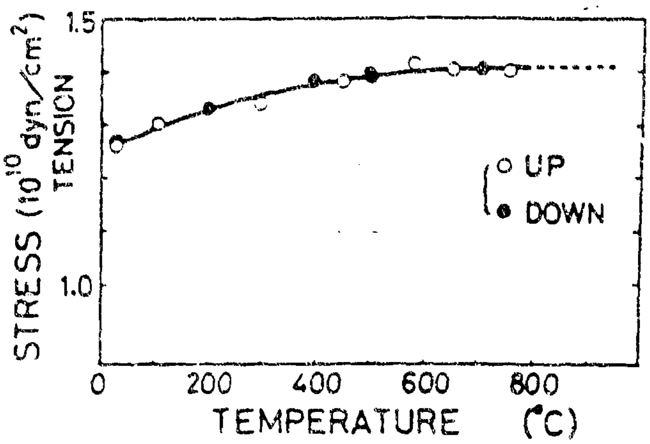

Fig. 5: Residual stress vs. temperature at measurement for increasing (up) and decreasing (down) temperatures.

Conditions: Gases: N_2, NH_3 and SiH_4; ϕNH_3 = 1000 cc/min;
T = 940 C; (100) Si wafer
Taken from Tamura [32]

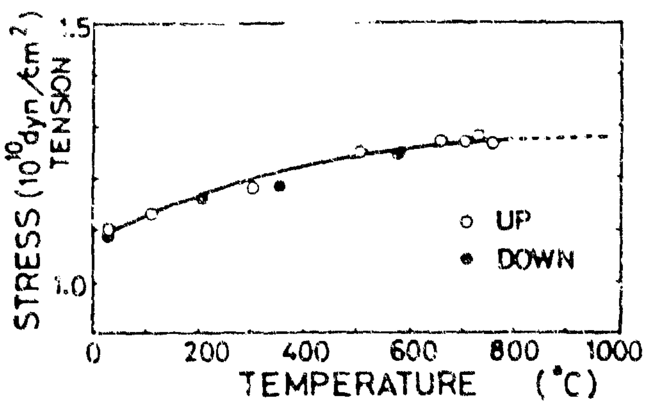

Fig. 6: Residual stress vs. temperature at measurement for increasing (up) and decreasing (down) temperatures.

Conditions: Gases: N_2, NH_3 and SiH_4; ϕNH_3 = 1000 cc/min;
T = 940 C; (111) Si wafer
Taken from Tamura [32]

Residual Stress

C.V.D.

Temperature - Residual Stress Relationships

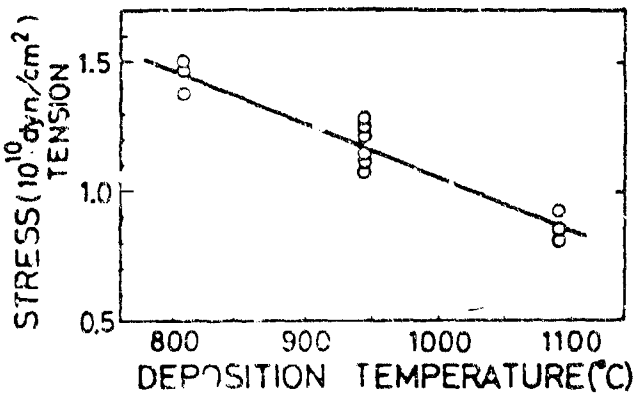

Fig. 7: Residual stress vs. deposition temperature.

Conditions: Gases: N_2, NH_3 and SiH_4; ϕNH_3 = 1000 cc/min; Taken from Tamura [32]

Residual Stress

A.P.C.V.D.

Annealing - Residual Stress Relationships

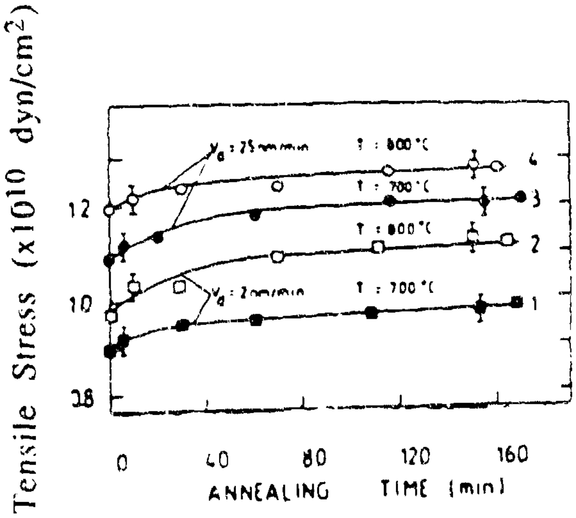

Fig. 8: The effect of annealing upon residual stress.

Conditions: Gases: Ar, NH_3 and SiH_4;SiH_4/NH_3 = 0.2
Net gas flow is constant; P = 133 Pa
Taken from Noskov [27]

Residual Stress

A.P.C.V.D.

Film Depth - Residual Stress Relationships

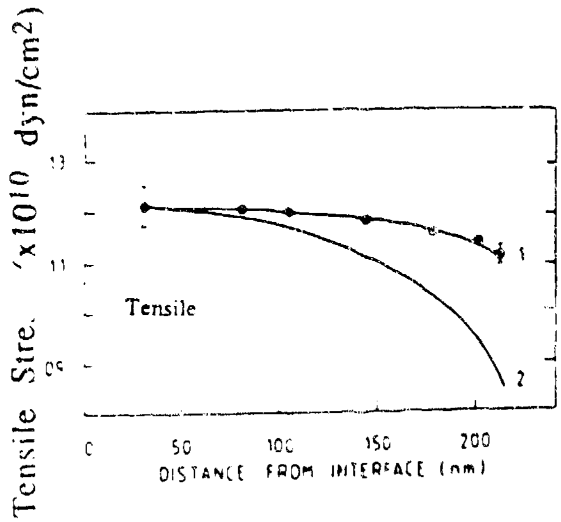

Fig. 9: Residual stress as a function of depth in film.

Conditions: Gases: Ar, NH_3 and SiH_4;SiH_4/NH_3 = 0.2
Net gas flow is constant; P = 133 Pa
Taken from Noskov [27]

Residual Stress

A.P.C.V.D.

Film Thickness - Residual Stress Relationships

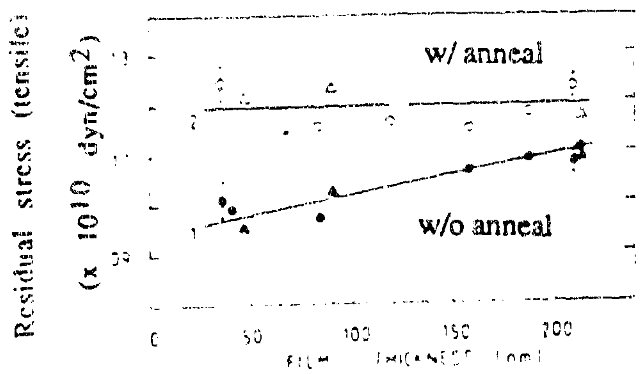

Fig. 10: Residual stress as a function of film thickness.

Conditions: Gases: Ar, NH_3 and SiH_4;SiH_4/NH_3 = 0.2
Net gas flow is constant; P = 133 Pa
Taken from Noskov [27]

Residual Stress

A.P.C.V.D.

Residual Stress Values

$(1.1 - 1.2) \times 10^{10}$ (dyn/cm^2) [27].

Conditions: Gases: Ar, NH_3 and SiH_4; $SiH_4/NH_3 = 0.2$;
Net gas flow is constant; P =133 Pa
Taken from Noskov [27]

Residual Stress

P.E.C.V.D.

Annealing - Residual Stress Relationships

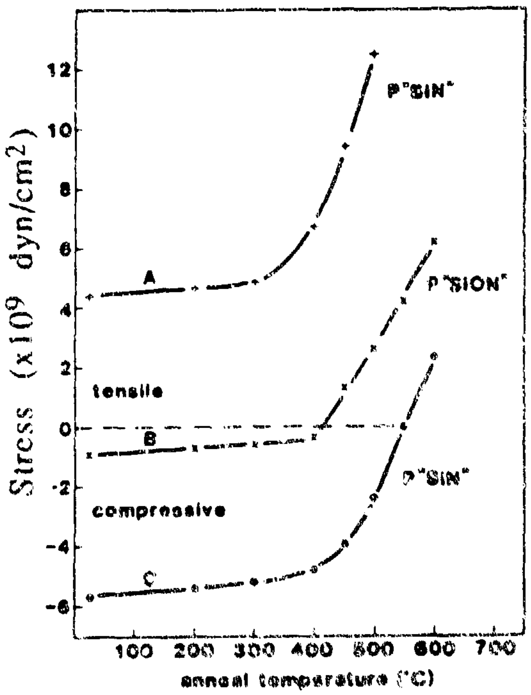

Fig. 1?: Residual stress vs. annealing temperature.

Conditions: Gases: N_2, NH_3 and SiH_4; ϕ_{NH3} = 1200 sccm;
ϕ_{SiH4} = 100 sccm; ϕ_{N2} = 200 sccm; R.F. frequency = 310 kHz
P = 130 Pa
Taken from Claassen [5]

Residual Stress

P.E.C.V.D.

Film Thickness - Residual Stress Relationships

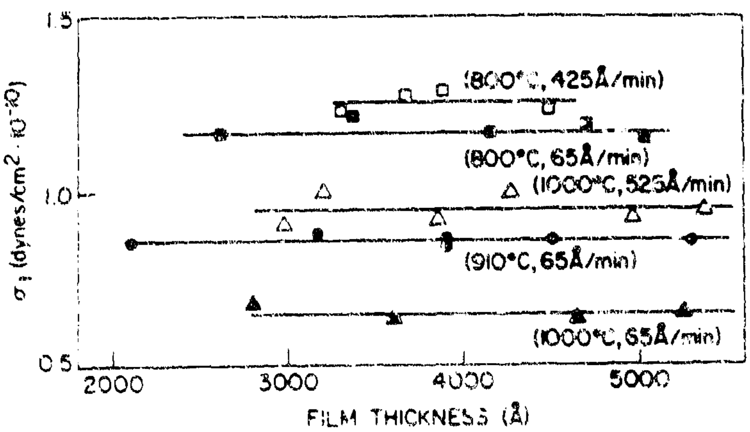

Fig. 12: Residual stress (tensile) as a function of film thickness.

Conditions: Gases: N_2, NH_3 and SiH_4; 1% SiH_4 in N_2;
NH_3/SiH_4 > 10; T - 800 - 1000 C
Taken from Irene [14]

Residual Stress

P.E.C.V.D.

Gas Flow - Residual Stress Relationships

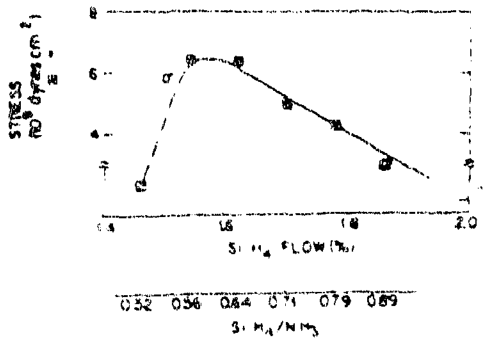

Fig. 13: Residual stress vs. SiH_4 flow and SiH_4/NH_3 ratio.

Conditions. Gases: Ar, NH_3 and SiH_4; SiH_4 conc. = 1.7%;
ϕ = 2320 sccm; R.F. power = 250 W;
P = 127 Pa; T = 275 C
Taken from Sinha [31]

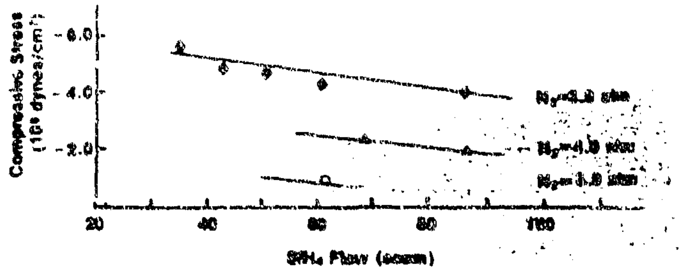

Fig. 14: Effect of SiH_4 flow upon residual stress.

Conditions: Gases: N_2, NH_3 and SiH_4; R.F. frequency = 13.56 MHz;
R.F. power = 300 -500 W; P = 267 - 668 Pa; T = 260 - 400 C
Taken from Cheng [3]

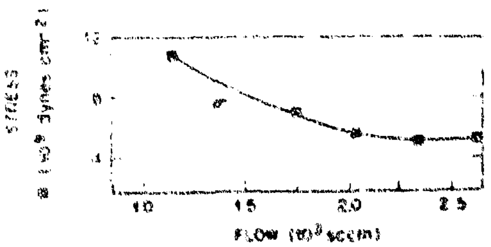

Fig. 15: Residual stress vs. net gas flow.

Conditions: Gases: Ar, NH_3 and SiH_4;
SiH_4/NH_3 = 0.71; R.F. power = 250 W;
P = 127 Pa; T = 275 C
Taken from Sinha [31]

Residual Stress

P.E.C.V.D.

Gas Flow - Residual Stress Relationships

Table 2 : Refractive index as a function of N_2O flow and Temperature.

N_2O flow (cm^3/min)	Temp. (C)	Compressive residual stress (10^9 dyne/cm^2)
0	200	3.6
10	200	3.7
30	200	3.0
60	200	2.0
90	200	1.2
0	250	3.0
10	250	2.3
30	250	1.6
60	250	0.9
90	250	1.0
0	300	3.1
10	300	2.3
30	300	1.2
60	300	0.7
0	350	2.1
10	350	0.5
20	350	0.3

<u>Conditions</u>: N_2, N_2O and NH_3; ϕ_{SiH4} (in N2) = 2950 cm^3/min;
R.F frequency = 380 kHz; R.F. power = 700 W, P = 48 Pa
Taken from Knolle [21]

Residual Stress

P.E.C.V.D.

Gas Ratios - Residual Stress Relationships

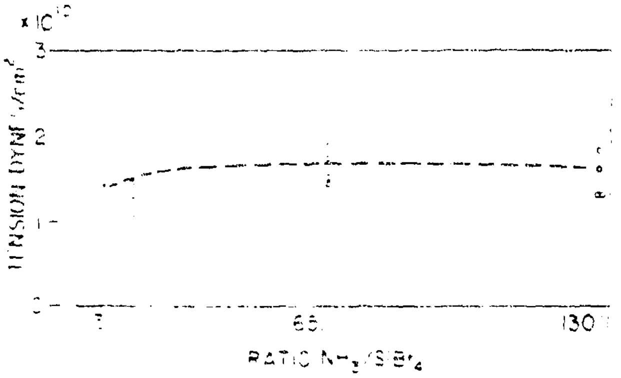

Fig. 16: Residual stress vs. $NH_3/SiBr_4$ ratio.

Conditions: Gases: NH_3 and $SiBr_4$; T = 800 C
Taken from Aboaf [1]

Fig. 17: Residual stress vs. $\%N_2$ in flow.

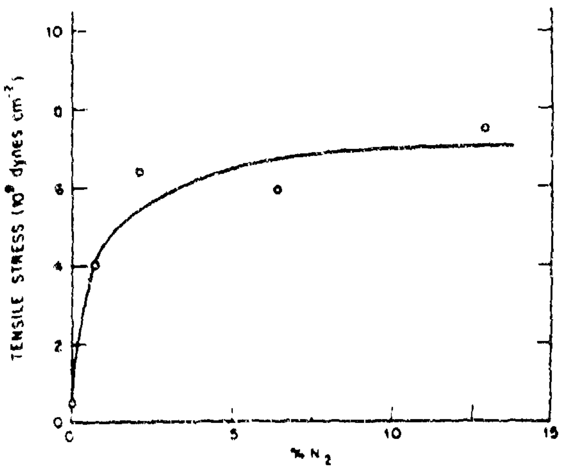

Fig. 17: Residual stress vs. $\%N_2$ in flow.

Conditions: Gases: Ar, N_2, NH_3 and SiH_4; SiH_4 conc. = 1.7%;
ϕ = 2320 sccm; R.F. power = 250 W;
P = 127 Pa; T = 275 C
Taken from Sinha [31]

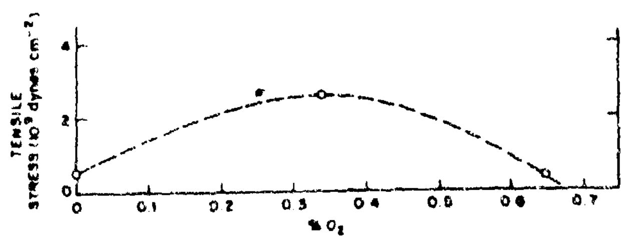

Fig. 18: The effect of O_2 addition on residual stress.

Conditions: Gases: Ar, NH_3, O_2 and SiH_4; SiH_4 conc. = 1.7%;
SiH_4/NH_3 = 0.71; ϕ = 2320 sccm; R.F. power = 250 W;
P = 127 Pa; T = 275 C
Taken from Sinha [31]

Residual Stress

P.E.C.V.D.

Gas Ratios - Residual Stress Relationships

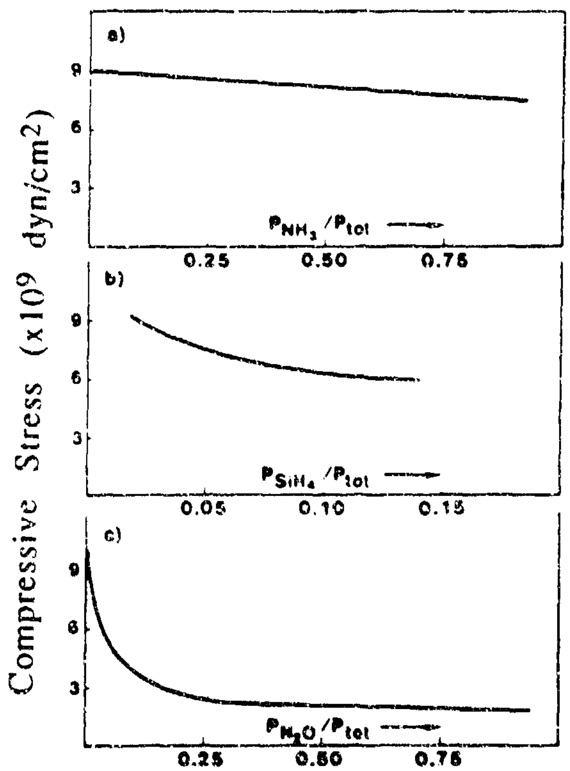

Fig. 19: Residual stress vs. partial pressures of component gases.

Conditions: Gases: N_2, NH_3 and SiH_4; R.F. frequency = 50 kHz;
P = 40 Pa; T = 300 C
Taken from Claassen [5]

Residual Stress

P.E.C.V.D.

Hydrogen Content - Residual Stress Relationships

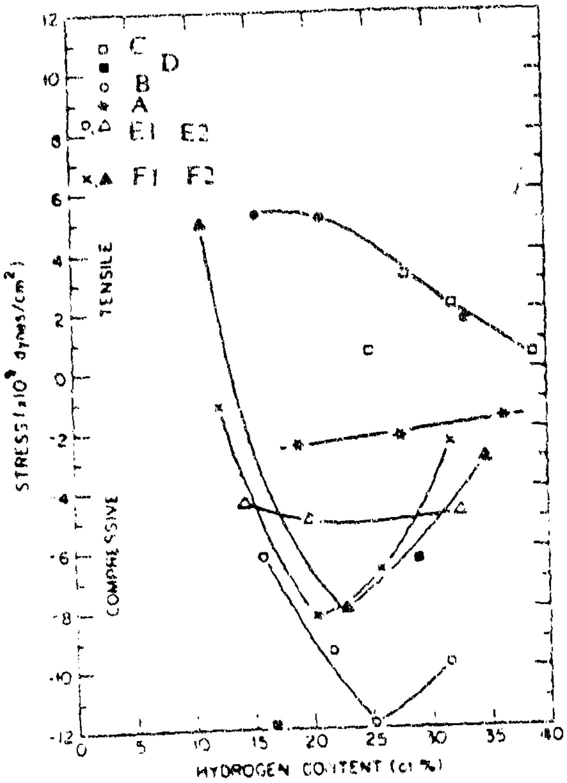

Fig. 20: Residual stress vs. hydrogen content.

Conditions: Gases: NH_3 and SiH_4;

System	frequency (Hz)	P (w/cm^2)	T (C)	Gas flow (sccm) SiH_4	NH_3	P (Pa)
A	13.56 MHz	0.04		?	?	40
B	13.56 MHz	0.38		22	80	56
C	13.56 MHz	0.02		17	120	42.7
D	187.5 kHz	0.06		1400	--	60
E1	50 kHz					
E2	450 kHz	150 W				
F1	50 kHz			333		280
F2	450 kHz			333		280

Taken from Kanicki [18]

Residual Stress

P.E.C.V.D.

Ion Implantation - Residual Stress Relationships

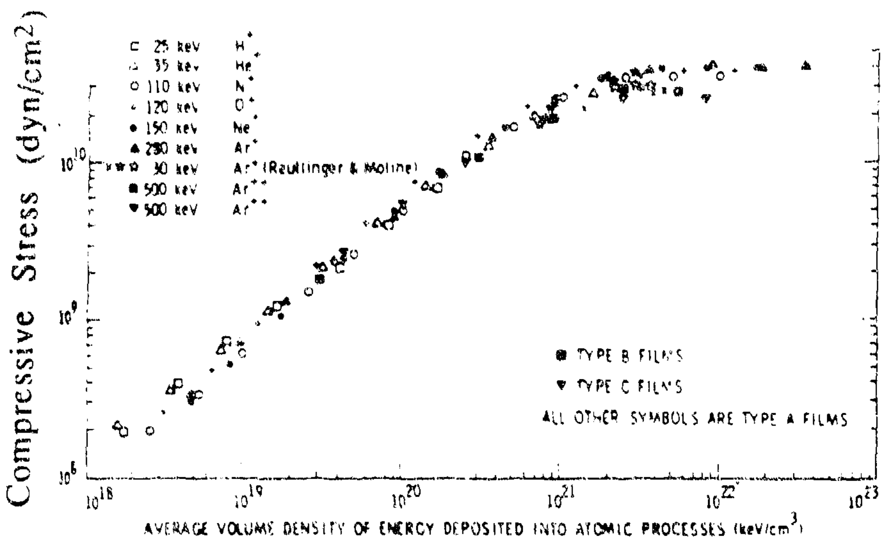

Fig. 21: Ion implantation induced residual compressive stress.

Conditions: Film A: 5% oxygen, T = 750 C, thickness = 2300 Angstroms
Film B: 0% oxygen, T = 750 C, thickness = 2000 Angstroms
Film C: 0% oxygen, T = 1000 C, thickness = 2000 Angstroms
Taken from Eernisse [10]

Residual Stress

P.E.C.V.D.

Refractive Index - Residual Stress Relationships

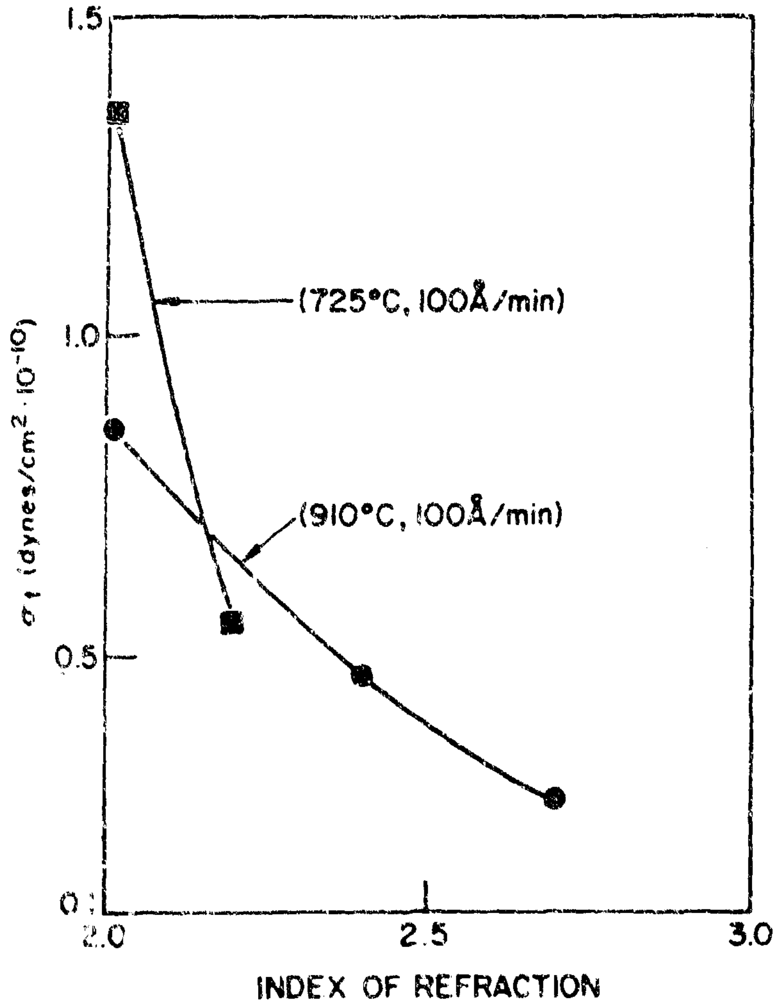

Fig. 22: Residual stress as related to refractive index.

Conditions: Gases: N_2, NH_3 and SiH_4 (1%); ϕ_{NH3} = 125 ml/min; ϕ_{SiH4} = 83 ml/min; NH_3/SiH_4 = 1?0. T = 725, 910 C
Taken from Irene [14]

Residual Stress

P.E.C.V.D.

R.F. Frequency - Residual Stress Relationships

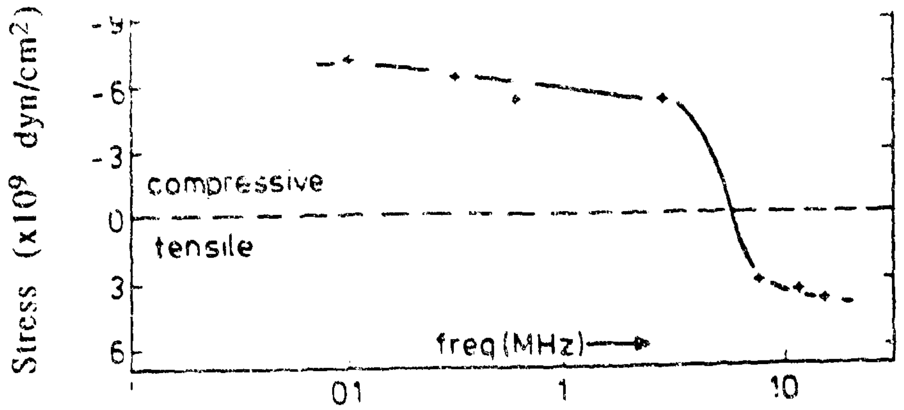

Fig. 23: Residual stress as a function of R.F. frequency.

Conditions: Gases: N_2, NH_3 and SiH_4; ϕ_{NH3} = 1200 sccm; ϕ_{SiH4} = 100 sccm; ϕ_{N2} = 200 sccm; P = 130 Pa
Taken from Claassen [6]

Residual Stress

P.E.C.V.D.

R.F. Power - Residual Stress Relationships

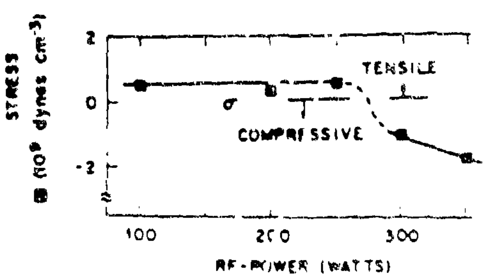

Fig. 24: Residual stress vs. R.F. power.

Conditions: Gases: Ar, NH_3, O_2 and SiH_4; SiH_4 conc = 1.7%; SiH_4/NH_3 = 0.71; ϕ = 2320 sccm; P = 127 Pa; T = 275 C
Taken from Sinha [31]

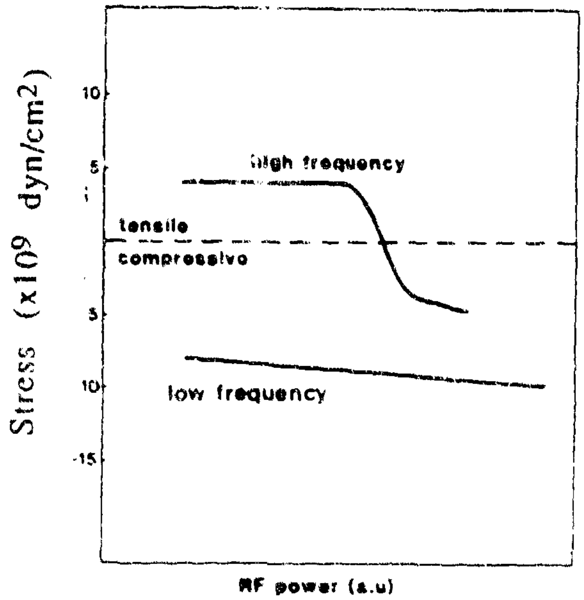

Fig. 25: Residual stress a a function of R.F. power.

Conditions: Gases: N_2, NH_3 and SiH_4; R.F. frequency = 50 kHz
P = 40 Pa; T = 300 C
Taken from Claassen [5]

Residual Stress

P.E.C.V.D.

Pressure - Residual Stress Relationships

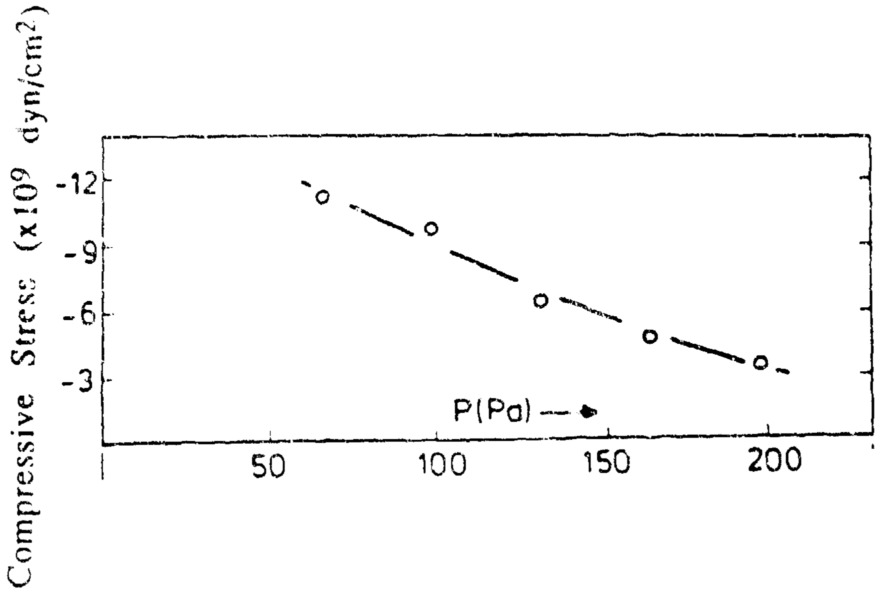

Fig. 26: Residual stress as a function of deposition pressure.

Conditions: Gases: N_2, NH_3 and SiH_4; ϕ_{NH3} = 1200 sccm; ϕ_{SiH4} = 100 sccm; ϕ_{N2} = 200 sccm; R.F. frequency = 310 kHz
P = 130 Pa
Taken from Claassen [6]

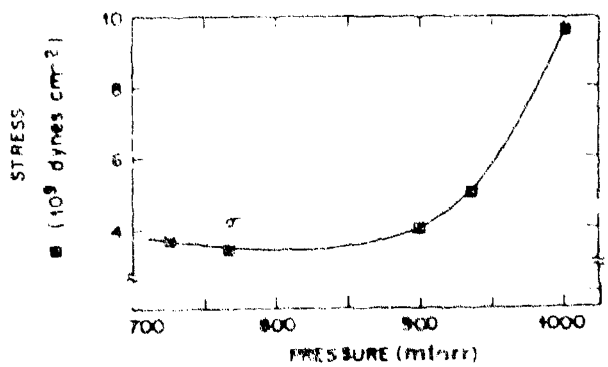

Fig. 27: Residual stress vs. pressure.

Conditions: Gases: Ar, NH_3, O_2 and SiH_4; SiH_4 conc. = 1.7%; SiH_4/NH_3 = 0.71; ϕ = 2320 sccm; T = 275 C
Taken from Sinha [31]

Residual Stress

P.E.C.V.D.

Temperature - Residual Stress Relationships

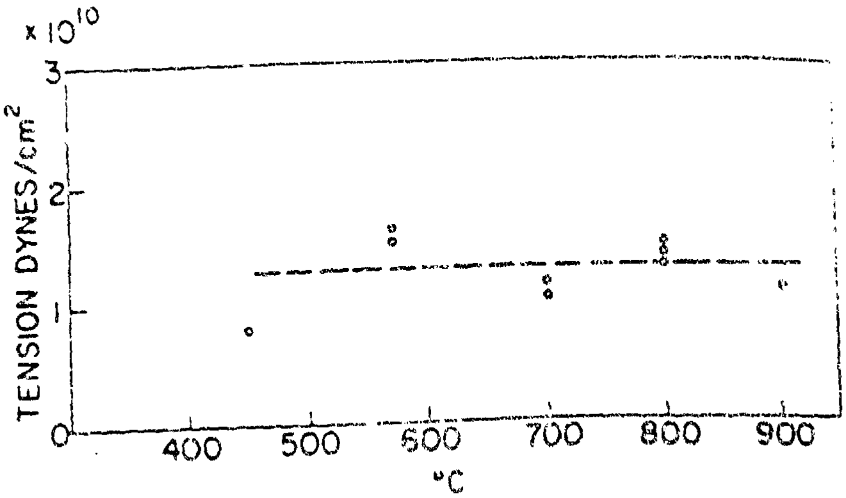

Fig. 28: Residual stress as a function of deposition temperature.

Conditions: Gases: NH_3 and $SiBr_4$: $SiBr_4/NH_3$ = 1:13;
T = 800 C
Taken from Aboaf [1]

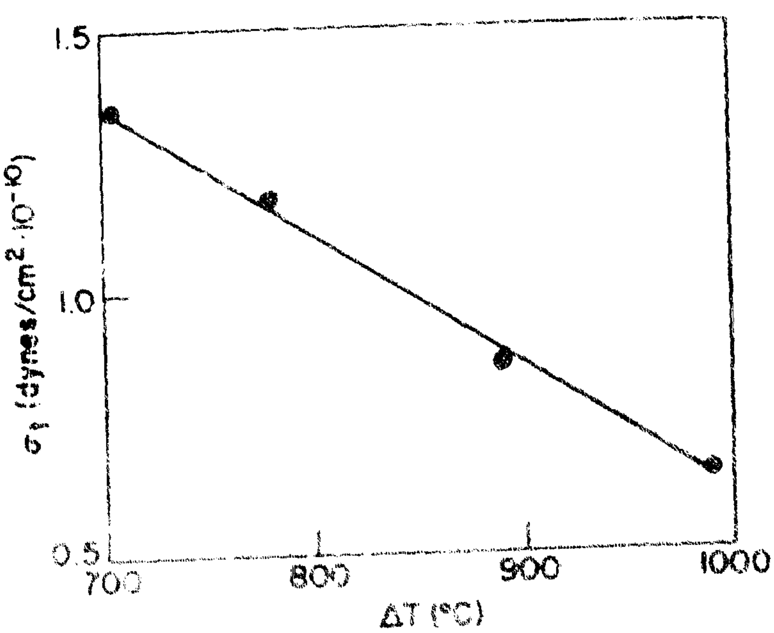

Fig. 29: Residual stress vs. (deposition - room) temperature.

Conditions: Gases: N_2, NH_3 and SiH_4 (1%); ϕ_{NH3} = 125 ml/min;
ϕ_{SiH4} = 83 ml/min; NH_3/SiH_4 = 150; T = 700 - 1000 C
Taken from Irene [14]

Residual Stress

P.E.C.V.D.

Temperature - Residual Stress Relationships

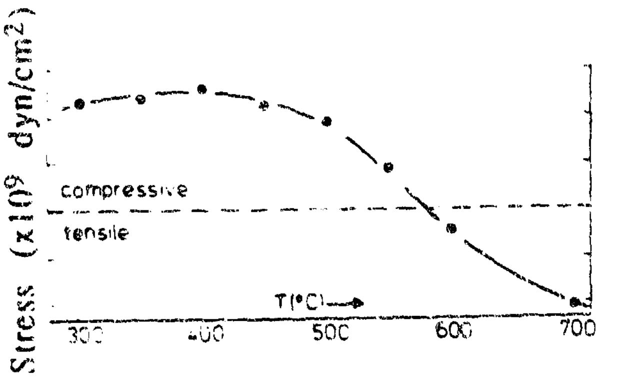

Fig. 30: Residual stress vs. deposition temperature.

Conditions: Gases: N_2, NH_3 and SiH_4; ϕ_{NH3} = 1200 sccm; ϕ_{SiH4} = 100 sccm; ϕ_{N2} = 200 sccm; R.F. frequency = 310 kHz
P = 130 Pa
Taken from Claassen [6]

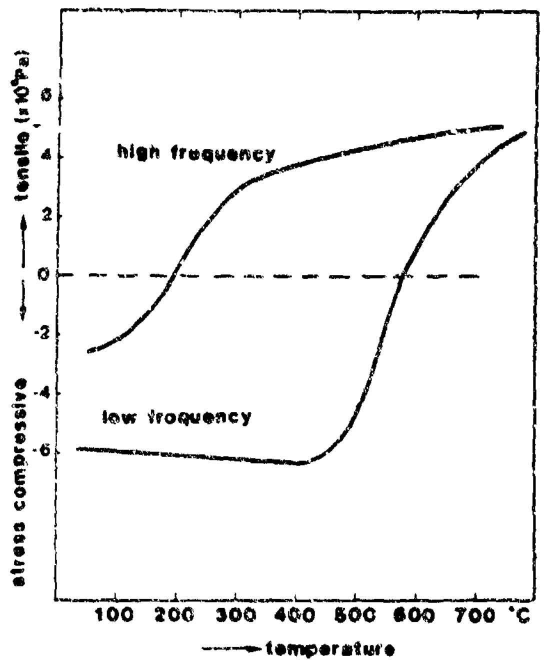

Fig. 31: Residual stress vs. deposition temperature.

Conditions: Gases: N_2, NH_3 and SiH_4; R.F. frequency = 50 kHz;
P = 40 Pa;
Taken from Claassen [5]

Residual Stress

P.E.C.V.D.

Temperature - Residual Stress Relationships

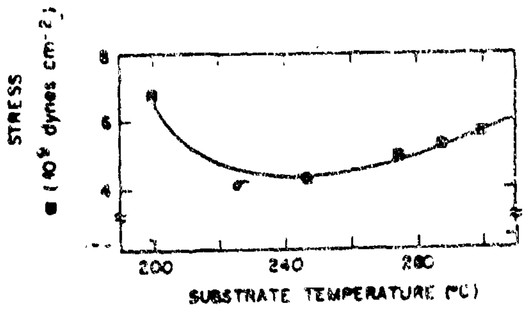

Fig. 32: Residual tensile stress vs. deposition temperature.

Conditions: Gases: Ar, NH_3, O_2 and SiH_4; SiH_4 conc. = 1.7%; SiH_4/NH_3 = 0.71; ϕ = 2320 sccm; P = 127 Pa; T = 275 C
Taken from Sinha [31]

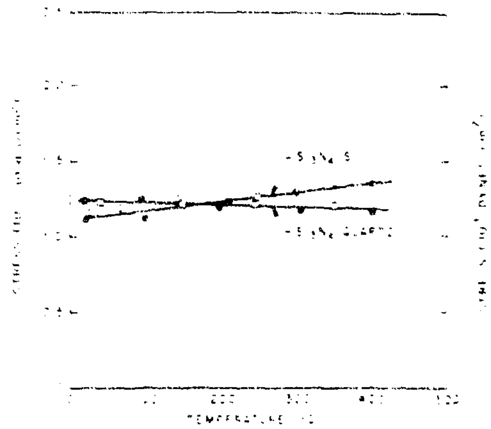

Fig. 33: Residual stress vs. deposition temperature for differing substrates.

Conditions: Nitrox plasma reactor
Taken from Retajczyk [29]

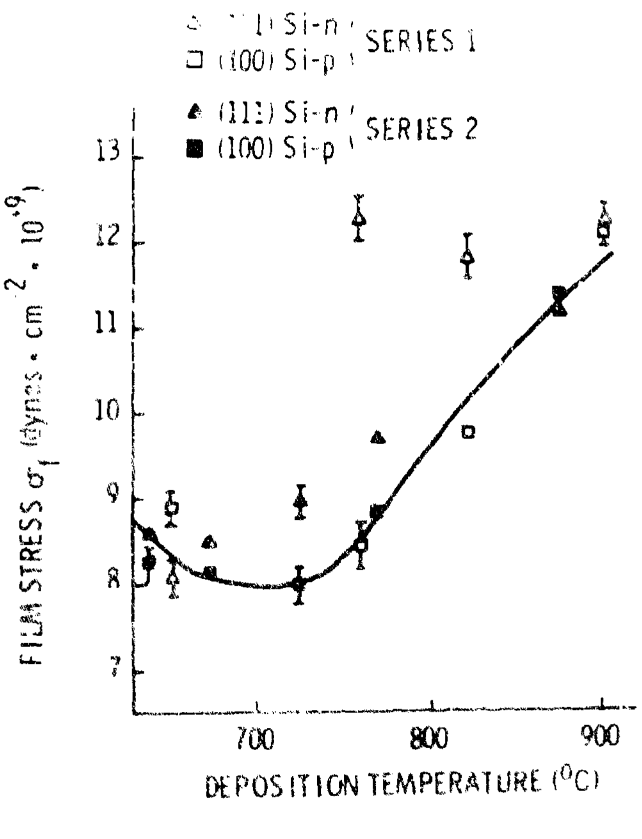

Fig. 34: Residual stress (tensile) vs. deposition temperature.

Conditions: Gases: N_2, NH_3 and SiH_4; NH_3/SiH_4 = 1000
Taken from Hezel [12]

Residual Stress

P.E.C.V.D.

Residual Stress Values

Table 3: Residual stress as a function of deposition parameters. [18]

System	f(Hz)	P_d (W cm^{-2})	T_s (°C)	P(T)	Gas Flow (sccm) SiH_4	NH_3	G_R (Å/min)	σx10^9 (dyn cm^{-2})
			120				170	-1.63
A	13.56 M	0.04	260	0.3	[illegible]	?	175	-2.17
			380				150	-2.47
			100				290	1.73
B	13.56 M	0.38	250	0.5	22	80	310	5.18
			370				320	5.28
			100				159	0.59
C	13.56 M	0.02	275	0.32	17	120	96	2.19
			320				--	2.14
			400				81	0.67
			100				140	-6.[illegible]
D	187.5 k	0.06	250	0.45	1400	--	112	-12.28
			350				141	-14.27
		150 W	100	0.6	380	1130	100	-9.85
			250	0.71	380	1705	89	-12.0
E1	50 k	235 W	380	1.49	365	2735	223	-9.41
			500	2.0	255	2945	218	-6.2
			100	0.6	380	1130	203	-4.84
E2	450 k	150 W	380	1.49	365	2735	212	-4.98
			500	2.0	245	2945	204	-4.34
		200 W	100			700	254	-2.51
		250 W	250			1525	239	-4.72
F1	50 k	300 W	380	2.1	333	2000	311	-8.03
		200 W	600			2400	398	-1.17
		300 W	100			700	288	-3.07
F2	450 k		380	2.1	333	2000	309	-7.18
		200 W	600			2400	369	0.54

Residual Stress

P.E.C.V.D.

Residual Stress Values

$(0.5 - 1.0) \times 10^{10}$ <Tensile> (dyn/cm^2) [19].

Conditions: Plasma Technology Model PD80 Reactor
Taken from Kember [19]

8.5×10^{9} <Tensile> (dyn/cm^2) [9].

Conditions: Gases. N_2, NH_3 and SiH_4; T = 700 - 900 C
Taken from Drum [9]

(8-11) $\times 10^{9}$ <Compressive> (dyn/cm^2) [7].

Conditions: Gases: N_2, NH_3 and SiH_4 (2%); ϕ_{N2} = 1575 cm^3/min; ϕ_{NH3} = 6 cm^3/min; ϕ_{SiH4} = 35 cm^3/min. R.F. power = 400 W;
R.F. frequency = 50 kHz; P = 33.3 Pa, T = 225 C
Taken from Dharmadhikari [7]

(7-9) $\times 10^{9}$ <Compressive> (dyn/cm^2) [7].

Conditions: Gases. N_2, NH_3 and SiH_4 (100%); ϕ_{N2} = 1000 cm^3/min; ϕ_{NH3} = 400 cm^3/min; ϕ_{SiH4} = 150 cm^3/min; R.F. power = 400 W;
R.F. frequency = 50 kHz; P = 26.7 Pa; T = 325 C
Taken from Dharmadhikari [7]

1.2×10^{10} <Tensile> (dyn/cm^2) [1].

Conditions: gases: NH_3 and $SiBr_4$; $SiBr_4/NH_3$ = 0.077;
T = 800 C
Taken from Aboaf [1]

Residual Stress

Sputtering

Composition and Temperature - Residual Stress Relationships

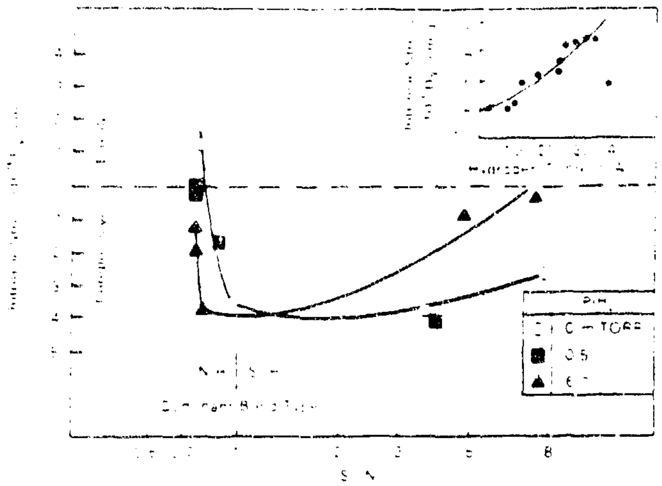

Fig. 35. Relationships between residual stress, Si/N ratio and hydrogen content.

Conditions: Gases: Ar, H_2 and N_2; R.F. power density = 3.29 W/cm^2;
T = 175 C
Taken from Martin [25]

Thermal Expansion Coefficient

C.V.D.

Thermal Expansion Coefficient Values

$2.5 - 3.85 \times 10^{-6}$ (1/C) [32].

Conditions: Gases: N_2, NH_3 and SiH_4;
T = 940 C
Taken from Tamura [32]

3.85×10^{-6} (C^{-1}) [34].

Conditions: Gases: SiH_4 and NH_3; T = 800 and 1000 C [34]

Thermal Expansion Coefficient

P.E.C.V.D.

Thermal Expansion Coefficient Values

1.6×10^{-6} (C^{-1}) [29].

Conditions: Nitrox Plasma Reactor; T = 800 C [29]

$\alpha_{Si3N4} - \alpha_{Si} = -9 \times 10^{-7}$ [14].

Conditions: Gases: SiH_4, NH_3 and N_2; 1% SiH_4 in N_2; $NH_3/SiH_4 > 10$; T = 700 - 1000 C [14]

Bulk Material

$(2.5 - 3.1) \times 10^{-6}$ (C^{-1}) [23].

Young's Modulus

C.V.D.

Young's Modulus Values

4.0×10^{12} (dyn/cm^2) [34].

Conditions: Gases: SiH_4 and NH_3; T = 800 and 1000 C [34]

Sputtering

Young's Modulus Values

1.3×10^{12} (dyn/cm^2) [22].

Korhonen [22] gave no details on the nitride processing used.

Bulk Material

$(2.96 - 3.03) \times 10^{12}$ (dyn/cm^2) [23].

References

1] Aboaf, J.A., "Some Properties of Vapor Deposited Silicon Nitride Films Obtained by the Reaction of $SiBr_4$ and NH_3", *J. Electrochem. Soc.* Vol. 116, No. 12(1969): 1736

2] Bromley, E.I., J.N. Randall, D.C. Flanders and R.W. Mount ?i., "A Technique for the Determination of Stress in Thin Films", *J. Vac. Sci. Technol. B*, Vol.1, No. 4(1983): 1364

3] Chang, Mei, Jerry Wong and David N.K. Wang, "Low Stress, Low Hydrogen, Nitride Deposition", *Solid State Technology*, May (1988): 193

4] Chow, Ray, W.A. Lanford, Wang Ke-Ming and Richard S. Rosler, "Hydrogen Content of a Variety of Plasma-deposited Silicon Nitrides", *J. Appl. Phys.*, Vol. 53, No. 8, (1982): 5630

5] Claassen, W.A.P., "Ion Bombardment-Induced Mechanical Stress in Plasma-Enhanced Deposited Silicon Nitride and Silicon Oxynitride Films", *Plasma Chemistry and Plasma Processing* Vol. 7, No. 1 (1987): 109

6] Claassen, W.A.P., G.J.N. Valkenburg, M.F.C. Willemsen and W.M. v. d. Wijgert, "Influence of Deposition Temperature, Gas Phase Composition, and RF Frequency on Composition and Mechanical Stress of Plasma Silicon Nitride Layers", *J. Electrochem. Soc.*, Vol. 132, No. 4 (1985): 893

7] Dharmadhikari, Vineet S., "Characterization of Plasma-deposited Silicon Nitride Coating Used for Integrated Circuit Encapsulation", *Thin Solid Films*, Vol. 153 (1987): 459

8] Doo, V.Y., D.R. Nichols and G.A. Silvey, "Preparation and Properties of Pyrolytic Silicon Nitride", *J. Electrochem. Soc.*, Vol. 113, No. 12 (1966): 1279

9] Drum, C.M. and M.J. Rand, "A Low-stress Insulating Film on Silicon by Chemical Vapor Deposition", *J. Appl. Phys.*, Vol. 39, No. 9 (1968): 4?58

10] EerNisse, E.P., "Stress in Ion-implanted C.V.D. Si_3N_4 films", *J. of Appl. Phys.*, Vol. 48, No. 8 (1977): 3337

11] Fate, W.A., "High-temperature Elastic Moduli of Polycrystalline Silicon Nitride", *J. Appl. Phys.*, Vol. 46, No. 6 (1975): 2335

12] R. Hezel and E.W. Hearn, "Mechanical Stress and Electrical Properties of MNOS Devices as a Function of the Nitride Deposition Temperature", *J. Electrochem. Soc.*, Vol. 125, No. 11 (1978):1848

13] Hirao, Takashi, Kentaro Setsune, Masatoshi Kitagawa, Takeshi Kamada, Kiyota Wasa and Tomio Izumi, "Influence of Deposition Conditions on the Properties of Silicon Nitride Films Prepared by the ECR Plasma CVD Method", *Jpn. Jrnl. Appl. Phys. 2, Lett.*, Vol. 26, No. 12(1987): 2015

14] Irene, E.A., "Residual Stress in Silicon Nitride Films", *Journal of Electronic Materials*, Vol. 5, No. 3 (1976): 287

15] Ishii, Yasunobu, Tatsuo Aoki and Shintaro Miyazawa, "Silicon Nitride Film Deposited by Hot-wall Plasma-enhanced CVD for GaAs LSI", *J.Vac. Sci. Technol. B*, Vol. 2, No. 1 (1984): 49

16] Isomae, S., Y. Tamaki, A. Yajima and M. Maki, "Dislocation Generation at Si_3N_4 Film Edges on Silicon Substrates and Viscoelastic Behavior of SiO_2 Films", *J. Electrochem. Soc.*, Vol. 126, No. 6 (1979): 1014

17] Jousse, D., J. Kanicki, D.T. Trick and P.M. Lenahan, "Electron-spin-resonance Study of Defects in Plasma-enhanced Chemical Vapor Deposited Silicon Nitride", *Appl. Phys. Lett.*, Vol. 52, No. 6 (1988): 445

18] Jerzy Kanicki and Nancy Voke, "Chemical and Mechanical Properties of Hydrogenated Amorphous Silicon Nitride Films Deposited in Various PECVD Systems", *Mat. Res. Soc. Symp. Proc.*, Vol. 68, (1986): 167

19] Kember, P.N., S.C. Liddell and P. Blackborrow, "Characterization of Plasma Deposited Silicon Nitride as Applied to Novel MOS Structures", *Semiconductor Int.*, Vol. 8, No. 8(1985): 8

20] Khaliq, M.A., Q.A. Shams, W.D. Brown and H. A. Naseem, "Physical Properties of Memory Quality PECVD Silicon Nitride", *Journal of Electronic Materials*, Vol. 17, No. 5 (1988): 355

21] Korhonen, A.S., P.L. Jones and F.H. Cocks, "On the Thermoelastic Properties of Hydrogenated Amorphous Silicon", *Materials Science and Engineering*, Vol. 49 (1981): 127

22] W.R. Knolle, J.W. Osenbach and A. Elia, "Nitride", *Journal of the Electrochemical Society*, Vol. 135, No.5 (1988): 1211

23] Kyocera Corporation, Mechanical and Industrial Ceramics, 1988.

24] Martin, P.M., "Summary Abstract: Relationships Between Stress and Local Hydrogen Bonding in Sputtered SiN:H",*J. Vac. Sci. Technol. A* 2 (2) (1984): 330

25] Martin, P.M. and G.J. Exarhos, " Summary Abstract: Relationships Between Stress, Composition, and Microstructure in Sputtered Silicon Nitride", *J. Vac. Sci. Technol. A* Vol. 3, No. 3 (1985): 615

26] Morosanu, C.E., "The Preparation, Characterization and Applications of Silicon Nitride Thin Films", *Thin Solid Films*, Vol. 65 (1980): 171

27] Noskov, E.B. Gorokhov, G.A. Sokolova, E.M. Trukhanov and S.I. Stenin, "Correlation Between Stress and Structure in Chemically Vapour Deposited Silicon Nitride Films", *Thin Solid Films*, Vol. 162 (1988): 129

28] Pan, Paihung and Wayne Berry, "The Composition and Physical Properties of LPCVD Silicon Nitride Deposited with Different NH_3/SiH_2Cl_2 Gas Ratios", *J. Electrochem. Soc.*, Vol. 132, No. 12 (1985): 3001

29] T.F. Retajczyck, Jr. and A.K. Sinha, "Elastic Stiffness and Thermal Expansion Coefficients of Various Refractory Silicides and Silicon Nitride Films", *Thin Solid Films*, Vol. 70 (1980): 241

30] Sekimoto, Misao, Hideo Yoshihara and Takeshi Ohkubo, "Silicon Nitride Single-Layer X-ray Mask", *J. Vac. Sci. Technol.*, Vol. 21, No. 4 (1982):1017

31] Sinha, A.K., H.J. Levinstein, T.E. Smith, G. Quinta[illegible] and S.E. Haszko, "Reactive Plasma Deposited Si-N Films for MOS-LSI Passivation", *J. Electrochem. Soc.*, Vol. 125, No. 4 (1978): 601

32] Tamura, Masao and Sunami, Hideo, "Generation of Dislocations Induced by Chemical Vapor Deposited Si_3N_4 Films on Silicon", *Japanese Journal of Applied Physics*, Vol. 11, No. 8 (1972): 1097

33] Tessier, Yves, J.E. Klemberg-Sapieha, S. Poulin-Dandurand and M.R. Wertheimer, "Silicon Nitride from Microwave Plasma: Fabrication and Characterization", *Canadian Journal of Physics*, Vol. 65 (1987): 859

34] Tokuyama, Takashi, Yasuhiro Fuji, Yoshimitsu Sugita and Seigou Kishino, "Thermal Expansion Coefficient of a Pyrolitically Deposited Silicon Nitride Film", *Japan. J. Appl. Phys.*, Vol. 6 (1967): 1252

35] Watanabe, Hideo, Kazuhisa Katoh and Shin-ichi Imagi, "Properties of Silicon Nitride Films Prepared by Plasma-enhanced Chemical Vapour Deposition of SiH_4-N_2 Mixtures", *Thin Solid Films*, Vol. 136, (1986):77

36] Zhou, Nan-Sheng, Shizuo Fujita and Akio Sasaki, "Structural and Electrical Properties of Plasma-deposited Silicon Nitride from SiH_4-N_2 Gas Mixture", *Journal of Electronic Materials*, Vol. 14, No. 1 (1985): 55